Charges, currents, and potentials in ionic channels of one conformation

Duanpin Chen and Robert Eisenberg

Department of Physiology, Rush Medical Center, Chicago, Illinois 60612 USA

ABSTRACT Flux through an open ionic channel is analyzed with Poisson–Nernst–Planck (PNP) theory. The channel protein is described as an unchanging but nonuniform distribution of permanent charge, the charge distribution observed (in principle) in x-ray diffraction. Appropriate boundary conditions are derived and presented in some generality. Three kinds of charge are present: (a) permanent charge on the atoms of the protein, the charge independent of the electric field; (b) free or mobile charge, carried by ions in the pore as they flux through the channel; and (c) induced (sometimes called polarization) charge, in the pore and protein, created by the electric field, zero when the electric field is zero. The permanent charge produces an offset in potential, a built-in Donnan potential at both ends of the channel pore. The system is completely solved for bathing solutions of two ions. Graphs describe the distribution of potential, concentration, free (i.e., mobile) and induced charge, and the potential energy associated with the concentration of charge, as well as the unidirectional flux as a function of concentration of ions in the bath, for a distribution of permanent charge that is uniform. The model shows surprising complexity, exhibiting some (but not all) of the properties usually attributed to single filing and exchange diffusion. The complexity arises because the arrangement of free and induced charge, and thus of potential and potential energy, varies, sometimes substantially, as conditions change, even though the channel structure and conformation (of permanent charge) is strictly constant. Energy barriers and wells, and the concomitant binding sites and binding phenomena, are outputs of the PNP theory: they are computed, not assumed. They vary in size and location as experimental conditions change, while the conformation of permanent charge remains constant, thus giving the model much of its interesting behavior.

INTRODUCTION

This paper describes the properties of simple models of open channels containing an unchanging arrangement of permanent charge, using the Poisson–Nernst–Planck theory (1–3) (PNP for short) to analyze channels containing permanent charge. The theory calculates the electric field, instead of assuming it (4–6).

This paper describes two types of permeating ions, say K^+ and Cl^-, flowing through a channel. Although the graphs presented illustrate the case of a uniform distribution of permanent charge, for the sake of simplicity, the theory applies also to a spatially nonuniform distribution of permanent charge, and such computations have been performed and reported in abstract (7).

Ions in a PNP theory are represented as points in a fluid, able to pass through each other; no ad hoc occupancy states or explicit interaction terms (involving the distance between individual ions) appear in the theory (although interactions occur through Poisson's equation). To our surprise, this (ridiculously) simple model can do many interesting things, even when the spatial arrangement of permanent charge is uniform: in particular, fluxes can have some of the properties of mediated and single-file transport, even though the conformation of the channel never changes and its ions are described as points that flow through each other.

Most studies of membrane transport (at least since the 1930s [6, 8, 9]) begin by comparing observed fluxes with a simple model, a system of one conformation, in which unidirectional fluxes are independent of each other (10–13). The fluxes observed in biology are rarely if ever independent, and so the simple model has usually been

replaced with more complex ones with multiple conformations and interactions. If unidirectional fluxes compete with each other, transport has been described as ions moving single file through a channel, ever since the measurements of Hodgkin and Keynes (14) of fluxes through the K^+ channel. If the unidirectional fluxes complement each other, transport has usually been described (since at least the measurements of Hodgkin and Keynes (15) on the Na^+ pump) as obligatorily linked in a cycle (16, 17); flux interactions are ascribed, somewhat mysteriously, to the cycle itself; to the conformational changes of the membrane proteins doing the transport, for example, the alternating conformations of ping-pong (18); or to occluded state models (19–21). The states of such models, and the rates of transition, are described by Markov models, akin to models of chemical kinetics, using the law of mass action, but the physical meaning of the rates and states is rather vague, as is their dependence on such parameters as channel diameter, length, dielectric coefficient or structure, or ionic composition and diffusion coefficient, or sometimes even concentration or membrane potential.

In these traditional paradigms the channel is (implicitly or explicitly) described as a spatial distribution of potential; and ions interact with this potential as they move through the channel pore. The distribution of potential is assumed constant as long as the protein is in a given conformation or state, although the source of charge and energy that maintains this potential is rarely specified. (Note that a molecule can maintain a constant spatial distribution of potential, as solutions and conditions change, only if charge is supplied to maintain that potential: Gauss' law [22]. Indeed, the amount of charge

---

Abbreviation used in this paper: PNP, Poisson-Nernst-Planck.

supplied must be different at different locations, if the spatial arrangement as well as the mean value is to remain constant.)

Our work suggests an alternative paradigm in which permeating ions interact with (just one) spatial distribution of permanent charge, unchanging as long as the protein is in a given conformation or state.[1] No energy is necessary to maintain this distribution of charge. But the spatial distribution of potential and energy cannot be constant in a system like this; it is determined by all the ions in the system. The potential and energy profile assume various shapes, determined by the field equations and boundary conditions, even though the permanent charge has just one conformation: the permanent charge does not move at all; free (and induced) charge does. It is the "conformations" of free and induced charge, more than anything else, that are responsible for the interesting phenomena of our model.

The Appendix presents the relevant field equations and derivation of their boundary conditions, because we cannot find them in physics texts (23, 24), which customarily pay little attention to distributions of permanent charge, discussing such in the context of electrets (25), if at all. The neglect of permanent charge, particularly in boundary conditions, is long standing, going back to Faraday and Maxwell (26-29), who were more confident of the existence of fields than charge, particularly permanent charge (according to historical analyses, see references 26-29; Buchwald [28] traces the development of the modern theory involving both permanent and induced charge).

The distribution of permanent charge is, of course, a central issue in chemistry texts (after all, the Hellman-Feynmann theorem ensures that electrostatics can describe much of chemistry [30]), but chemistry books usually do not present the field equations and boundary conditions at all, and when they do (31, 32), they are not in the form we need.

This paper uses a one-dimensional description of the channel (Eqs. 33-37), depending on earlier work (1-3) for derivation and mathematical justification. The one-dimensional description has such simple physical meaning that it seems a robust and inescapable approximation to the full three-dimensional problem: it can be viewed here as the beginning of a physical theory, the PNP theory, justified by physics, rather than the end of a mathematical theory, derived by asymptotics.[2]

The reader most interested in using the PNP theory

---

[1] To belabor an important point, in this paper the protein remains in just one state through all transport processes, even when concentrations or membrane potential change drastically. The state and conformation of the protein are defined in this paper as the distribution of permanent charge $P(z)$.

[2] However, the precise form of the variable $\tilde{\varepsilon}$ of Eq. 33 et seq. and its dependence on ϵ and α must be determined by mathematics, as far as we can see.

should turn immediately to the section "The physiological case . . ." near Eq. 14.

THEORY

Asymptotic analysis

The fundamentally three-dimensional equations presented in the Appendix can be reduced to a one-dimensional system, much easier to integrate, using asymptotic analysis (3), but now including permanent charge as well as space charge and induced charge along the channel wall. This analysis is too involved to recapitulate here, so reference is made to the earlier papers, which solved a similar problem but without permanent charge. The new boundary condition (Eq. A29) replaces the boundary condition (3.19) of reference 3. Most of the asymptotic analysis is unchanged; in particular, the boundary conditions and expansions for potential, the "switchback" term in the near field, and the matching between far field $\Psi(z, r, \theta)$ and near field $\phi(z, r, \theta)$ are not changed by the presence of permanent charge, nor are the boundary conditions, differential equations, expansions, or explicit expressions for the concentration profiles $C_j(z)$. The asymptotic process $\alpha \to 0$ is now the "distinguished limit" (33) $\alpha \to 0$, $\varepsilon \to 0$, $\omega_0 \to 0$, with $\tilde{\varepsilon}$, $\tilde{\omega}_0$, and λ^2 fixed, where

$$\tilde{\varepsilon} \equiv \frac{\varepsilon}{-\alpha^2 \cdot \ln \alpha} = O(1)$$

$$\tilde{\omega}_0(z) \equiv \frac{\omega_0(z)}{\alpha^2} = O(1). \tag{1}$$

The order notation: $O(1)$ means "of order one as $\alpha \to 0$" (see Olver [reference 34, p. 4-11]).

The permanent charge at the boundary does make one important change. The new jump condition (Eq. A25) adds an extra term to Eqs. 5.9 and 5.14 of reference 3, generalizing their modified Poisson equation.

$$\frac{d^2\Phi(z)}{dz^2} = \overbrace{-2\tilde{\omega}_0(z)}^{\substack{\text{Permanent} \\ \text{charge}}} \overbrace{- 2\tilde{\varepsilon}[\Delta(1 - z) - \Phi(z)]}^{\substack{\text{Dielectric correction:} \\ \text{induced charge}}} \overbrace{- \tilde{q}(z)}^{\substack{\text{Free} \\ \text{charge}}}, \tag{2}$$

where

$$\tilde{q}(z) = \lambda^2 \sum_j \frac{z_j C_j(z)}{I_c} = \frac{ed^2}{\epsilon_{1r}\epsilon_0 \cdot kT} q(z). \tag{3}$$

Here $\Phi(z)$ is the asymptotic approximation to the dimensionless potential $\Phi(z) \sim \phi(z, r, \theta) = [e/kT] \cdot \varphi(x, r, \theta)$ where $\varphi(x, R, \theta)$ is the (three-dimensional) potential with units volts of Eq. 6; $C_j(z)$ (units: $1/m^3$) is the approximation to the three-dimensional concentration $c_j(x, r, \theta)$; Δ is the potential across the channel, the transmembrane potential, inside minus outside (i.e., left minus right) in dimensionless units; and $\lambda = \kappa d$ is the channel length in units of the Debye length κ^{-1}, where

$\kappa^2 = e^2 \bar{I}_c/(\varepsilon_{r1}\epsilon_0 \cdot kT)$, with the ionic strength $\bar{I}_c$ (units: m^{-3}) computed from the ionic strength in either the left- or right-hand bath. Dimensionless units were defined in Eq. A27 and the ionic strength is

$$I_c(L) = \tfrac{1}{2}C_L \sum_j l_j z_j^2; \quad I_c(R) = \tfrac{1}{2}C_R \sum_j r_j z_j^2. \quad (4)$$

The free charge (i.e., space charge carried by ions) $\tilde{q}(z)$ is, of course, determined by the distribution of concentration, namely, the solution of the Nernst–Planck equations (Eqs. A4–A6 or 14 and 15). This solution can be determined by direct integration (cf. Eq. 5.7 of reference 3)

$$C_j(z) = \frac{l_j C_j(0)e^{z_j\Delta} \int_z^1 \dfrac{e^{z_j\Phi(\zeta)}}{D(\zeta)}\,d\zeta + r_j C_j(1) \int_0^z \dfrac{e^{z_j\Phi(\zeta)}}{D(\zeta)}\,d\zeta}{e^{z_j\Phi(z)} \int_0^1 \dfrac{e^{z_j\Phi(\zeta)}}{D(\zeta)}\,d\zeta}. \quad (5)$$

Eqs. 2 and 5 together form the integrodifferential equation, which, with boundary conditions, describes the one-dimensional approximation to a pore in a dielectric, the PNP theory. Most of the boundary conditions follow easily from an asymptotic analysis of Eqs. A7–A10, but the relation between the potentials and concentrations on the left and right side of the channel $\Phi(z = 0)$, $\Phi(z = 1)$, $C_j(0)$, and $C_j(1)$, and the potentials and concentrations far away in the bath, will require more discussion later, because of the presence of permanent charge and the concomitant built-in Gibbs–Donnan potential (4), i.e., the potential often called a surface potential or double-layer potential in the Debye–Hückel or Gouy–Chapman theory (35, 36).

The differential equations and boundary conditions together determine the fluxes of individual ions, which can be written explicitly after direct integration of the Nernst–Planck equations (Eqs. A4–A10).

$$J_j = J_j(L \to R) - J_j(R \to L)$$
$$= \frac{C_j(0)e^{z_j\Phi(0)}}{\int_0^1 \dfrac{e^{z_j\Phi(z)}}{D_j(z)}\,dz} - \frac{C_j(1)e^{z_j\Phi(1)}}{\int_0^1 \dfrac{e^{z_j\Phi(z)}}{D_j(z)}\,dz}. \quad (6)$$

The terms on the right-hand sides of Eq. A6 are the unidirectional fluxes in obvious notation; $\Phi(1)$ is included explicitly for later reference, although at the moment it is zero. This expression can be derived or computed from many forms of stochastic analysis or simulations (equations 2.24 and 7.5 of reference 37; Eisenberg, Klosek, and Schuss, personal communication). Note that if the potential function depends on the original location of the ions (i.e., the side from which they enter the channel), the notation would need to be changed and the denominators of the right-hand side would differ.

It is interesting then to look at the homo- or self-flux ratio, the ratio of unidirectional fluxes of the same ion, which is widely used as a measure of coupling, using the

reasonable (but not necessarily true) assumption that an ion entering the channel from the inside interacts with the same potential function $\Phi(z)$ as an ion entering from the outside,

$$\frac{J_j(L \to R)}{J_j(R \to L)} = \frac{C_j(0)e^{z_j\Phi(0)}}{C_j(1)e^{z_j\Phi(1)}}. \quad (7)$$

More complex expressions arise if the diffusion coefficient and/or potential function are different for the two unidirectional fluxes.

The ratio of fluxes of different ions, the hetero- or mixed-flux ratio, must be written more carefully, because the potential function is almost certainly not the same for different types of ions (see Discussion). For example (one case out of four),

$$\frac{J_k(L \to R)}{J_j(R \to L)} = \frac{C_k(0)e^{z_k\Phi_k(0)}}{C_j(1)e^{z_j\Phi_j(1)}} \cdot \frac{\int_0^1 \dfrac{e^{z_k\Phi_k(z)}}{D_k(z)}\,dz}{\int_0^1 \dfrac{e^{z_j\Phi_j(z)}}{D_j(z)}\,dz}. \quad (8)$$

The electric potential $\Phi(z)$ of these equations is determined by the modified Poisson equation (Eq. 32), which depends on the concentrations $C_j(z)$ as well as the surface charge (remembering $\varepsilon_{r2} \ll \varepsilon_{r1}$):

$$-\varepsilon_{r1}\epsilon_0 \frac{d^2\Phi(z)}{dz^2}$$

$$= \frac{2}{a} \overbrace{[\sigma_0(z)}^{\substack{\text{Permanent} \\ \text{charge}}} + \overbrace{\varepsilon_{r2}[\sigma_2(z) - \sigma_1(z)]]}^{\substack{\text{Induced} \\ \text{charge}}} + \overbrace{\tilde{q}(z)}^{\substack{\text{Free} \\ \text{charge}}}. \quad (9)$$

Boundary conditions and the built-in potential

The analysis just given requires knowledge of the potential Φ on either end of the channel. The channel contains permanent charge, however, and so in general the potentials at the interface between pore and bath are not equal to the potentials far away in the bath, namely, the potentials measured and/or controlled experimentally. The potential in the pore contains a built-in component, a Donnan potential, present even when flux is zero, because the concentration of ions close to the channel is not equal to that far away, as a necessary consequence of the permanent charge within the channel. (Otherwise, the permanent charge in the channel would produce a continuing current.)

The built-in potential can be described and analyzed by field equations and boundary conditions similar to those used for the channel pore. We are less interested in the bath than the channel and so have not yet done such analysis. Rather, we follow the treatment of the built-in potential in a metal–semiconductor junction (38–40), which is essentially similar to the analysis of the equilibrium double layer in electrochemistry or physiology (4,

35, 36, 41). Both assume that the solutions in the bath are large enough in volume, total content, and concentration of all ions that fluxes into the channel do not disturb the equilibrium distribution of concentration and potential (in the baths). We have been reminded by our collaborators that further study of the entry process is needed, using a hierarchy of analyses, viz., macroscopic analysis of nonstationary phenomena, like accumulation and depletion (V. Barcilon, personal communication); mesoscopic analysis of ion–ion interactions (M. Ratner, Z. Schuss, and M. Klosek, personal communication); and simulations of all atomic motions (R. Elber and D. Rojewska, personal communication).

The equilibrium distribution in the baths occurs when all fluxes are negligible,

$$0 = J_j = D_j \left\{ \frac{dC_j}{dz} + z_j C_j \frac{d\Phi}{dz} \right\} \quad \text{for} \quad \left\{ \begin{array}{l} z < 0 \\ \text{or} \\ z > 1 \end{array} \right. \quad (10)$$

The differential equation and boundary conditions have the solution,

$$C_j(z_j, z) = C_j(L)e^{-z_j\Phi(z)} \quad z < 0$$

$$C_j(z_j, z) = C_j(R)e^{-z_j\Phi(z)} \quad z > 1. \quad (11)$$

Here $C_j(L)$ and $C_j(R)$ are the concentration of one of the ions on the Left at $z = -\infty \equiv L$ or on the Right at $z = +\infty \equiv R$, far away from the mouth of the channel. When there is no flux, the electrochemical potential is surely the same on both sides of the left-hand (or the right-hand) pore/bath interface; the electrical potential is the same[3]; and the concentration of each species is the same. Then, the modified Poisson equation (Eq. 2) implies

$$\sum z_j C_j (z = 0) + P(z = 0) = 0 \quad \text{at} \quad z = 0 \quad (12)$$

$$\sum z_j C_j (z = 1) + P(z = 1) = 0 \quad \text{at} \quad z = 1. \quad (13)$$

The form of the equations in our further analysis depends on the ionic composition of the bathing solutions, so we consider the simplest special case in this paper, switching to a more explicit, hopefully more accessible notation.

Physiological case: two univalent ions

Consider a solution made from two univalent ions (e.g., KCl) and write the concentrations that depend on location as $K(z)$ and $Cl(z)$. The Nernst–Planck equations become

$$J_K = -D_K \left\{ \frac{dK}{dz} + K \frac{d\Phi}{dz} \right\} \quad 0 < z < 1 \quad (14)$$

$$J_{Cl} = -D_{Cl} \left\{ \frac{dCl}{dz} - Cl \frac{d\Phi}{dz} \right\} \quad 0 < z < 1, \quad (15)$$

---

[3] In our treatment dipoles at the interfaces are described as part of the permanent charge $P(x, r, \theta)$ of Eq. A2.

where $\Phi(z)$ is determined by the modified Poisson equation, written here with all its sources, the charges on the right-hand side, and the unknown potentials on the left-hand side,

$$\frac{d^2\Phi(z)}{dz^2} - 2\tilde{\epsilon} \cdot \Phi(z) = -2\tilde{\omega}_0(z) - 2\tilde{\epsilon}(1 - z)\Delta$$

$$- \frac{\lambda^2}{l_c}(K(z; \Delta) - Cl(z; \Delta)). \quad (16)$$

We include the transmembrane potential Δ in the list of arguments of the concentrations to emphasize their dependence on the potential across (and in, for that matter) the pore. Eqs. 10 and 11 imply

$$K(0) \cdot Cl(0) = K(L) \cdot Cl(L)$$

$$K(d) \cdot Cl(d) = K(R) \cdot Cl(R), \quad (17)$$

where $K(L) = Cl(L)$ are the concentrations of K^+ and Cl^- in the left bath far from the channel; $K(R) = Cl(R)$ are the concentrations in the right bath far from the channel. From Eq. 41

$$K(0) - Cl(0) + P(0) = 0. \quad (18)$$

Taken together, Eqs. 11, 17, and 18 determine the built-in potential

$$\Phi_{bi}(0) = \ln \frac{P(0) + \sqrt{P^2(0) + 4[K(L)]^2}}{2K(L)}, \quad (19)$$

which is written for only the left-hand side of the channel. The concentrations at the left-hand side of the pore are then

$$K(0) = -\tfrac{1}{2}P(0) + \sqrt{\tfrac{1}{4}P^2(0) + [K(L)]^2} \quad (20)$$

$$Cl(0) = \tfrac{1}{2}P(0) + \sqrt{\tfrac{1}{4}P^2(0) + [K(L)]^2}. \quad (21)$$

Of course,

$$K(0) = K(L)e^{-\Phi_{bi}(0)}$$

$$Cl(0) = Cl(L)e^{\Phi_{bi}(0)}. \quad (22)$$

Experimentally, potentials are measured and/or applied in the left-hand bath $\Phi(L)$ or the right-hand bath $\Phi(R)$. Thus, the potential within the channel is not equal to the applied potential but is rather offset by the Donnan potential

$$\Phi(0) = \Phi_{bi}(0) + \Phi(L)$$

$$\Phi(1) = \Phi_{bi}(1) + \Phi(R) = \Phi_{bi}(1), \quad (23)$$

where $\Phi(L)$ is the experimentally controlled potential and we choose the zero of potential according to physiological convention, far away on the outside (right) of the channel $\Phi(R) \equiv 0$.

The net flux of K^+ is independent of the built-in potentials and vanishes at the equilibrium potential for K^+,

as it must in the two-ion case to satisfy thermodynamic constraints.[4]

$$J(K^+; \text{net}) = \frac{K(L)e^{\Phi(L)}}{\int_0^1 \frac{e^{\Phi(K^+;z)}}{D(K^+; z)} dz} - \frac{K(R)}{\int_0^1 \frac{e^{\Phi(K^+;z)}}{D(K^+; z)} dz} \quad (24)$$

using the fact that the potential far away from the channel, i.e., $\Phi(L)$ or $\Phi(R)$, is independent of the species of ion. Analogous expressions describe $J(Cl^-; \text{net})$.

Note that the net flux will not vanish at the equilibrium potential if the diffusion coefficient and/or potential function are different for the two unidirectional fluxes. Evidently, $\Phi(0)$ and $\Phi(1)$ can have such dependence only if they can be sources of energy, at least in this two-ion case.

The homo-flux ratios are also independent of the built-in potentials and show no sign of "single filing" or "exchange diffusion" behavior.

$$\frac{J(K^+; L \to R)}{J(K^+; R \to L)} = \frac{K(L)e^{\Phi(L)}}{K(R)} . \quad (25)$$

The hetero-flux ratios are illustrated by

$$\frac{J(Cl^-; R \to L)}{J(K^+; L \to R)} = \frac{Cl(R)e^{\Phi(L)}}{K(L)} \cdot \frac{\int_0^1 \frac{e^{\Phi(K^+;z)}}{D(K^+; z)} dz}{\int_0^1 \frac{e^{-\Phi(Cl^-;z)}}{D(Cl^-; z)} dz} . \quad (26)$$

Note that the flux ratio depends on the profiles of the concentration, and potential, as well as the diffusion coefficients, although it does not depend on the built-in potential.

In this simple case of two ions, the unidirectional influx and efflux depend on the *trans* concentration of the moving ion (the external concentration for efflux, the internal concentration for influx), although such dependence is not thought to be a property of Nernst–Planck equations. The coupling occurs through the built-in potential, which changes $\Phi(0)$ and $\Phi(1)$, the potential at the end of the channel. Those potentials are affected by the total concentration of ions on each side of the channel. The built-in potential modifies the potential within the channel, thus directly affecting the electrical component of unidirectional flux. The potential also modifies the concentration of ions within the channel, thus affecting the diffusive component of unidirectional flux. The system is thoroughly coupled and fluxes show some, but not all, of the dependence usually ascribed to single filing or exchange diffusion, as we shall see further in Results.

---

[4] These have not been explicitly included in our model, which is kinetic, not thermostatic, and thus we must check that flux and current vanish when the driving force vanishes.

MATERIALS AND METHODS

The modified Poisson equation (Eq. 16) and the Nernst–Planck equations (Eqs. 14–15) are solved by the nonlinear block iteration method shown by workers on semiconductors to have very good convergence (p. 61 of Mock [38]), using the discrete spatial variable $z[i]$ where i is an index running from 0 through $N + 1$, and the (forward) increment $h[i]$ in z defined by

$$h[i] \equiv z[i + 1] - z[i]. \quad (27)$$

The Nernst–Planck equations are solved analytically (see Eq. 5) with the equilibrium boundary conditions (Eqs. 22–23), rather than by iteration (as in the semiconductor literature) because the analytical solution improves accuracy and speed by dramatically improving convergence. The integrals in Eq. 5 must be evaluated for each x and so we use the trapezoidal rule: the more elaborate rules we have used elsewhere (37) are less efficient in this case.

The modified Poisson equation (Eq. 16) becomes in obvious notation, using the index m to count the iteration,

$$\frac{1}{\lambda^2} \frac{\dfrac{\Phi[i + 1; m + 1] - \Phi[i; m + 1]}{h[i]} - \dfrac{\Phi[i; m + 1] - \Phi[i - 1; m + 1]}{h[i - 1]}}{\dfrac{h[i] + h[i - 1]}{2}}$$

$$= -P[i] + Cl[i, m] + (Cl[i + 1, m] - Cl[i, m])$$

$$\times \mathbb{F}(\Phi[i + 1, m] - \Phi[i, m]) + (Cl[i - 1, m] - Cl[i, m])$$

$$\times \mathbb{F}(\Phi[i - 1, m] - \Phi[i, m]) - K[i, m] - (K[i + 1, m]$$

$$- K[i, m]) \cdot \mathbb{F}(\Phi[i, m] - \Phi[i + 1, m]) - (K[i - 1, m]$$

$$- K[i, m]) \cdot \mathbb{F}(\Phi[i, m] - \Phi[i - 1, m]) \quad (28)$$

where

$$\mathbb{F}(\zeta) \equiv \begin{cases} {}^1\!/_6 & \text{for } z = 0 \\ \dfrac{e^\zeta - 1 - \zeta - {}^1\!/_2\zeta^2}{\zeta^2(e^\zeta - 1)} & \text{for } z \neq 0. \end{cases} \quad (29)$$

To avoid metastasis of sub- and superscripts, we write the indexes of discretized functions as arguments of the function, within brackets, e.g., $\Phi[i, m]$. Note that the permanent charge is allowed to vary with position.

The numerical solution is started with a guess of the potential profile $\Phi(z) \leftrightarrow \Phi[i, m = 0]$, which is used to determine $C_j(z) \leftrightarrow C_j[i, m = 0]$ from Eqs. 5, 22, and 23. $\Phi[i, m = 1]$ is then determined by Eq. 24. That profile is then used to determine $C_j[i, m = 1]$, and the iteration goes on until the solutions converge as required. Our initial guess is usually a linear profile $\Phi(z)$ ranging from one built-in potential $\Phi_{bi}(0)$ to the other $\Phi_{bi}(L)$. We search for multiple solutions to the system, corresponding in principle to open and closed states of the channel (7) by iterating from other initial guesses $\Phi(z) \leftrightarrow \Phi[i, m = 0]$, within the physiological domain of $-20 < \Phi(z) < 20$, i.e. potentials of less than some 0.5 V in magnitude. The existence of multiple solutions to this system of equations has been shown both analytically and numerically (42–44).

RESULTS

Two ions, uniform charge

We begin with the simple case of two ions, say K^+ and Cl^-, in a channel with uniform charge density, understanding full well that more complex arrangements of charge are present in most channels, and are needed to fit most data sets. The channel of Fig. 1 has diameter 4 Å, length 45 Å, and is bathed on the left, the inside, with 100 mM KCl; the potential difference was 100 mV, inside positive, unless otherwise stated, and qualitative properties were independent of potential as checked in the range -300 to $+300$ mv. The solution on the right varies from 1 mM to 10 M (which is, we know, only possible in the computer). The diffusion coefficient $D_K = 10^{-6}$ cm²/s and $D_{Cl} = 10^{-9}$ cm²/s. The dielectric coefficient of the pore is $\varepsilon_{r1} = 80$, that of the channel protein is $\varepsilon_{r2} = 2$. In Fig. 1 A the channel contains a uniform permanent charge density corresponding to $P(z)$ of six negative charges per channel, making a permanent charge (volume) density of 18 M, or surface charge density of 1.1 charge/nm². In Fig. 1 B, a channel with (otherwise) the same parameters is assigned a much lower uniform charge density, $\sim 1/15 \simeq 0.067$ positive charges per channel, making a volume density of 200 mM, so the fluxes are reasonable in value. (More positive charge densities reduce the flux because they exclude the more mobile ion, the counterion, the cation.)

These charge densities are reasonable because channel walls are made of proteins, strings of covalently linked atoms, and "most covalently bonded atoms carry partial charges" (p. 30 of Schulz and Schirmer [45]). For example, each oxygen and each nitrogen of the peptide bond link has a net partial charge of some -0.4 (unit: charge on protons), each C' carbon (of the carbonyl moiety) has a net partial charge of $+0.5$; even one of the hydrogens (the H_N on the nitrogen) has a significant charge, $+0.2$. The distances between these charges are very small (bond lengths here being some 1–1.3 Å) and so the energies produced by these charges are large. Salt bridges (also called ionic bonds or coulomb interactions) made of such charges at distances of even 5 Å have energies of several kT and have large effects on rates (i.e., fluxes) that vary as $\exp\{\text{energy}/kT\}$.

Fig. 1 shows that as the external concentration of K^+ is increased, the unidirectional efflux, namely, $J_K(L \to R)$ of Eq. 37, changes, depending on the sign of the permanent charge. This coupling might well be interpreted traditionally as the result of single filing, when $P(z) < 0$, or exchange diffusion, when $P(z) > 0$, since a Nernst–Planck equation, with a potential profile independent of $[K^+]_{out}$, would predict an efflux independent of $[K^+]_{out}$.

The question is, How does this coupling occur in a model like ours, with a channel of just one conformation, containing ionic points able to flow through each other?
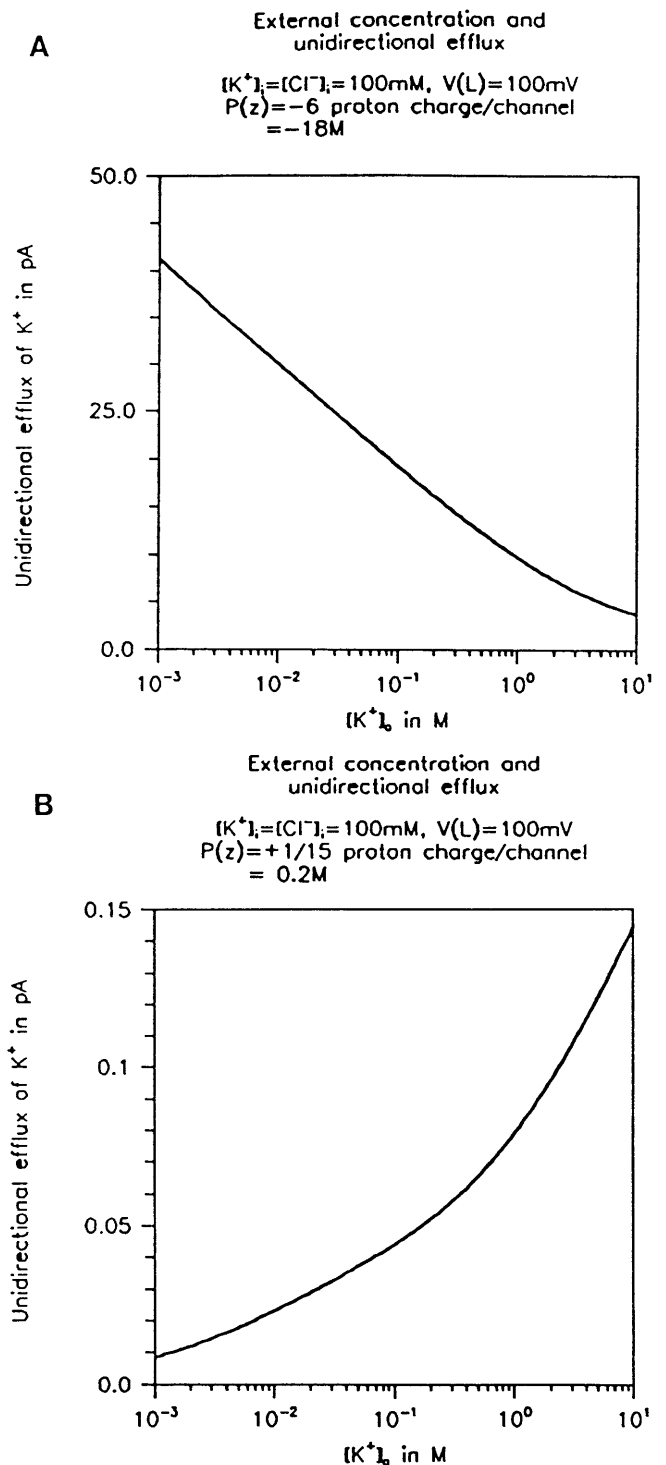
A

External concentration and
unidirectional efflux

$[K^+]_i=[Cl^-]_i=100$mM, $V(L)=100$mV
$P(z)=-6$ proton charge/channel
$=-18$M

B

External concentration and
unidirectional efflux

$[K^+]_i=[Cl^-]_i=100$mM, $V(L)=100$mV
$P(z)=+1/15$ proton charge/channel
$= 0.2$M

FIGURE 1 Unidirectional efflux and external concentration. Unidirectional fluxes in Nernst–Planck equations (e.g., Eqs. 6 and 27 of text) are often said to be independent of the *trans* concentration. If the channel protein is described as a uniform distribution of permanent charge, the distribution of potential within the channel depends on *trans* concentration, and therefore so does the unidirectional flux. If the permanent charge is negative and uniform, the efflux decreases with increasing *trans* concentration (A), as in traditional models of single filing. If the permanent charge is positive and uniform, it increases with increasing *trans* concentration (B), as in traditional models of exchange diffusion. The parameter values are described in the text.

Negative cation channels are shown in the next set of figures. The profiles of concentration for two different $[K^+]_{out}$, 1 mM and 1 M, are illustrated in Fig. 2. The average slope changes sign, of course, as the equilibrium potential for K^+ changes sign. Note that the permanent charge $P(z) \simeq K(z)$, the positive ionic charge; as expected, the channel is filled predominantly with counterions K^+. Cl^- is present in little concentration; it has less mobility, and contributes a tiny flux, but its concentration must not be set identically to zero, particularly if the permanent charge is positive. The potential profiles (not shown) are nearly straight lines, for both $[K^+]_{out} = 1$ mM and 1 M, as might be guessed from the PNP analysis of electric fields in channels without permanent charge (3), but the values of the potential are quite different, reflecting the dramatically different values of the built-in potential: $\Phi_{bi}(0) = -139$ mV; $\Phi_{bi}(1) = -254$ mV in the 1-mM solution and $\Phi_{bi}(0) = -139$ mV; $\Phi_{bi}(R) = -75$ mV in the 1-M solution.

The induced and net charges also change dramatically with concentration, as shown in Fig. 3, as does the profile of potential energy density $V(z)$ (units: joules/m^3) shown in Fig. 4, A and B, defined as

$$V(z) \equiv \rho(z)(\Phi(z) - \Phi_{bi}(1)), \qquad (30)$$

where $\rho(z)$ is the net charge (density) defined by Eqs. A1 and A2, including the (uniform) permanent charge density $P(z)$, as well as the induced and ionic (i.e., free or mobile) charge. Interestingly, the potential energy function $V(z)$ shows a clear minimum in this case, although the potential profile does not. (Nor does the permanent charge density, which is uniform, as in all the calculations of this paper.)

The potential energy density $V(z)$ is probably the best descriptor of binding of ions in a macroscopic model like this because it, not the potential, is the variable that describes the potential energy of a macroscopic concentration of ions in a region of the pore. $\Phi(z)$ describes the potential energy of one ion. The binding site does not appear in the potential $\Phi(z)$ or in the permanent charge density (which is uniform here), only in $V(z)$; thus, one should examine the potential energy function $V(z)$ when seeking qualitative understanding, when considering the "equivalent" structures, conformations, or states of channels, widely used in intuitive analyses of permeation. A separate analysis shows that the components of potential energy (as opposed to the net potential energy, V) do not have such interesting properties or structure, at least in this case.

The current–voltage relation expected from such an open channel is remarkably linear (not shown) as are many current–voltage relations of open channels, but variation in slope conductance and reversal potential with concentration are not characteristic of real channels (not shown). More complex arrangements of perma-
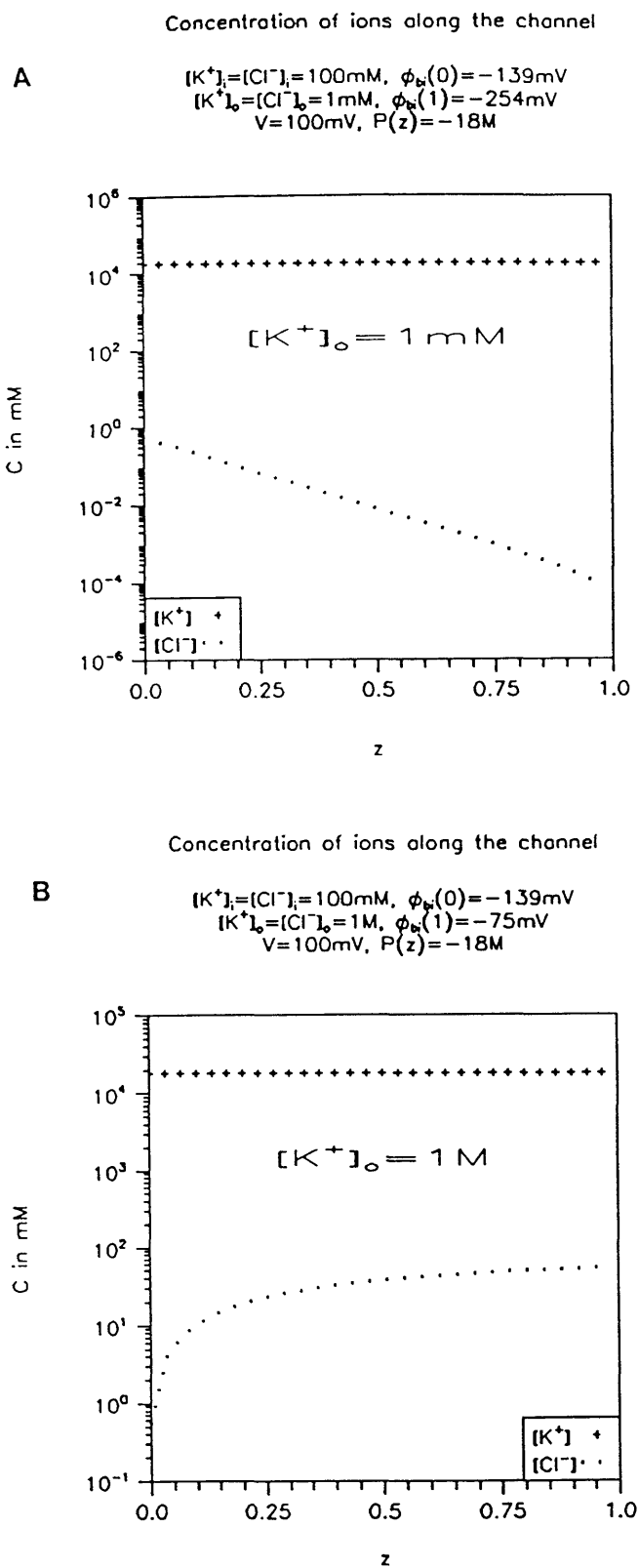
Concentration of ions along the channel

A

$[K^+]_i=[Cl^-]_i=100mM$, $\phi_{bi}(0)=-139mV$
$[K^+]_o=[Cl^-]_o=1mM$, $\phi_{bi}(1)=-254mV$
$V=100mV$, $P(z)=-18M$

Concentration of ions along the channel

B

$[K^+]_i=[Cl^-]_i=100mM$, $\phi_{bi}(0)=-139mV$
$[K^+]_o=[Cl^-]_o=1M$, $\phi_{bi}(1)=-75mV$
$V=100mV$, $P(z)=-18M$

FIGURE 2 Concentration profile along a channel of uniform negative permanent charge with external concentrations of 1 mM (A) and 1 M (B). Other parameters are described in text. The simplicity of the curves reflects the simplicity of the assumed structure of permanent charge. More complex structures produce much more complex behavior (7).
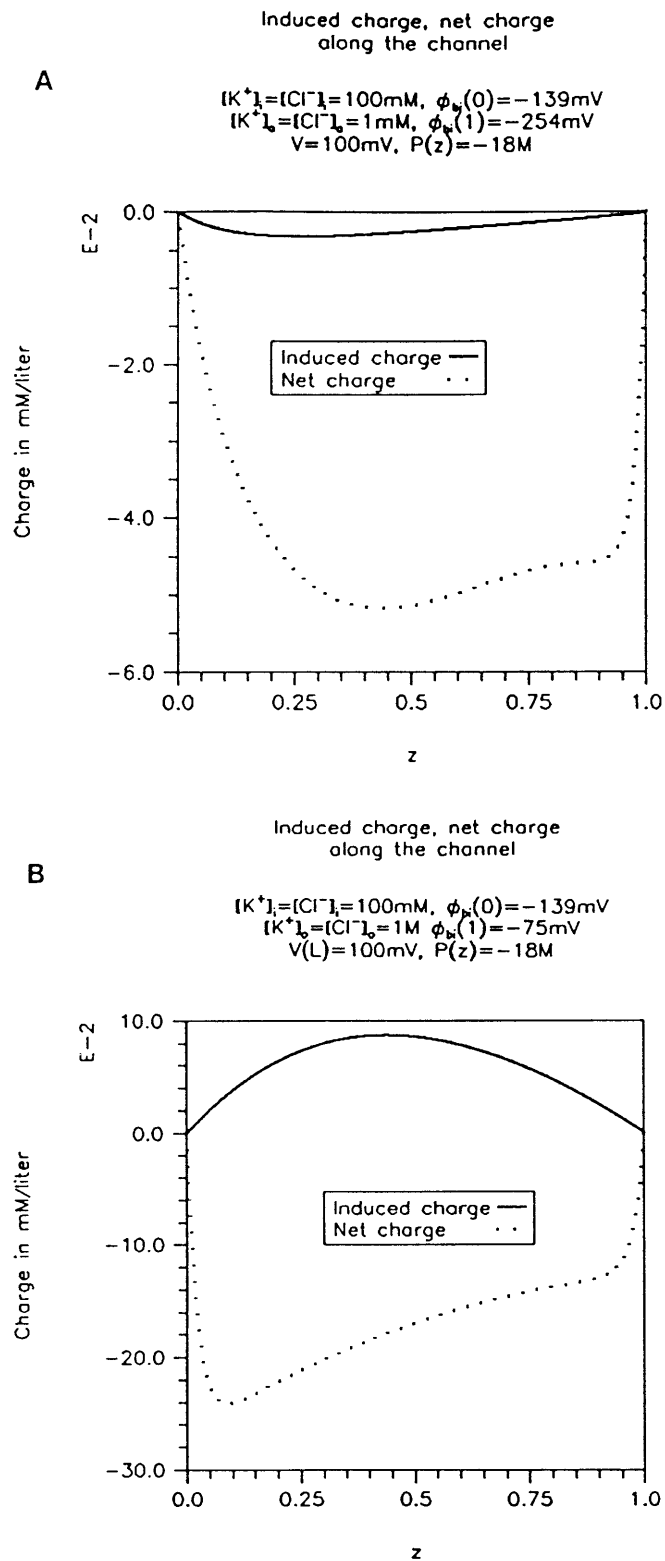
Induced charge, net charge along the channel

A

$[K^+]_i=[Cl^-]_i=100mM$, $\phi_{bi}(0)=-139mV$
$[K^+]_o=[Cl^-]_o=1mM$, $\phi_{bi}(1)=-254mV$
$V=100mV$, $P(z)=-18M$

Induced charge ——
Net charge · · ·

Potential energy density V(z)

A

$[K^+]_i=[Cl^-]_i=100mM$, $[K^+]_o=[Cl^-]_o=1mM$
$\phi_{bi}(0)=-139mV$, $\phi_{bi}(1)=-254mV$
$V(L)=100mV$, $P(z)=-18M$

$[K^+]_o = 1\ mM$

Induced charge, net charge along the channel

B

$[K^+]_i=[Cl^-]_i=100mM$, $\phi_{bi}(0)=-139mV$
$[K^+]_o=[Cl^-]_o=1M$ $\phi_{bi}(1)=-75mV$
$V(L)=100mV$, $P(z)=-18M$

Induced charge ——
Net charge · · ·

Potential energy density V(z)

B

$[K^+]_i=[Cl^-]_i=100mM$, $[K^+]_o=[Cl^-]_o=1M$
$\phi_{bi}(0)=-139mV$, $\phi_{bi}(1)=-75mV$
$V(L)=100mV$, $P(z)=-18M$

$[K^+]_o = 1\ M$

FIGURE 3   Induced charge and net charge along a channel of uniform negative permanent charge with external concentrations of 1 mM (A) and 1 M (B). Other parameters are described in text. Note that the induced charge is quite significant with external concentration of 1 M and the different curves for net charge are quite different in that case.
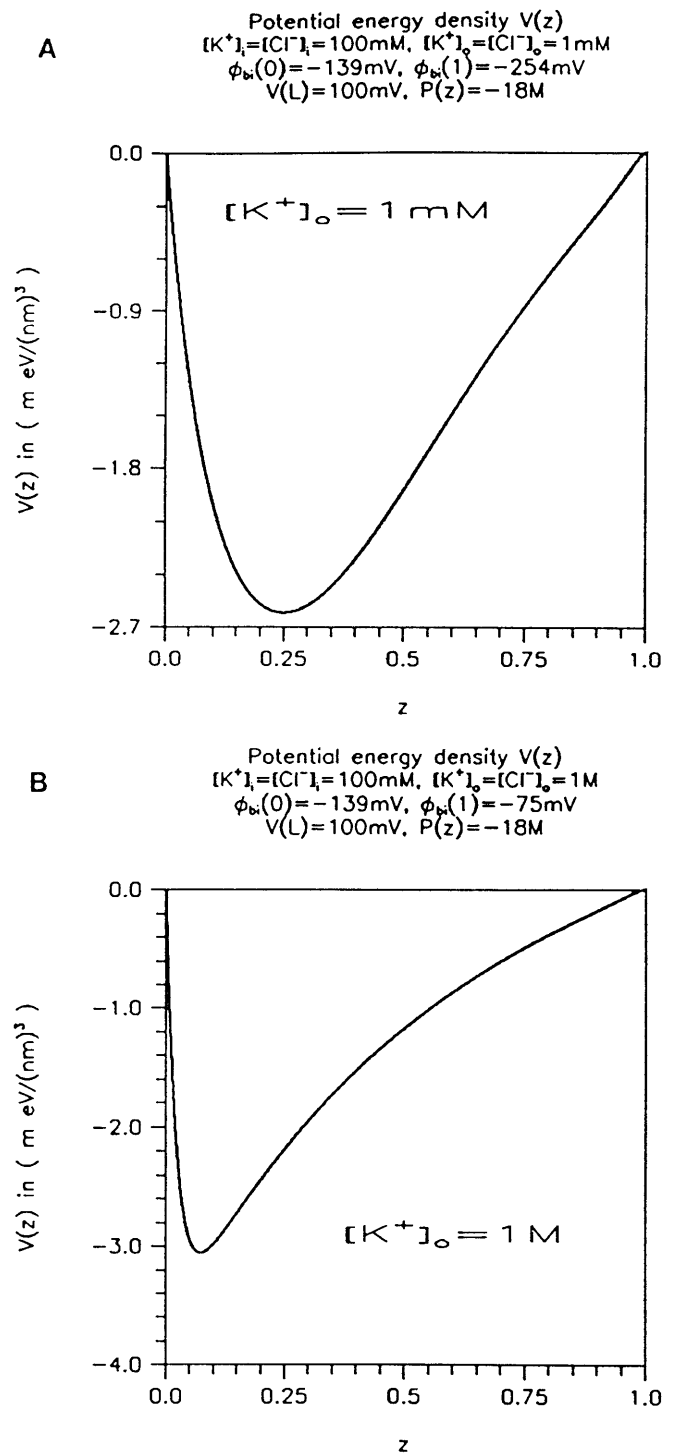
FIGURE 4   The net potential energy density $V(z)$ of the charge stored in the channel of uniform negative permanent charge with external concentrations of 1 mM (A) and 1 M (B). Other parameters are described in text. The energy of binding of this concentration of ions $V(z)$ depends on the external concentrations. The potential $\Phi(z)$ measures the energy of binding one ion. It too depends on external concentrations, but not so markedly as $V(z)$, because $V(z) = \rho(z)[\Phi(z) - \Phi_{bi}(1)]$ and the density of charge $\rho(z)$ also depends on external concentration.

nent charge give properties more characteristic of real channels.

Two ions, uniform positive charge

Fig. 5 illustrates the distribution of potential with a positive charge density $P(z) = 0.2$ M; Fig. 6 shows the resulting distribution of concentration. Note the qualitative difference in the curves at 1 mM and 1 M, one well below the fixed charge density, one well above it, unlike in Fig. 2. Fig. 7 gives the distribution of induced and net charges, showing the significance of all types of charge. Fig. 8 shows a marked dependence of the potential energy profile $V(z)$ on concentration, while Fig. 9 shows a dramatic conversion from a barrier in net potential energy $V(z)$ to a well, as concentration is raised. Plots of current–voltage relations, and conductance and reversal potential versus concentration (not shown), are nonlinear, as are similar properties of real channels.

It is clear that distributions of free charge and net potential energy $V(z)$ in the pore change dramatically with conditions, even in our simple model with uniform charge, provided the channel protein is described as an arrangement of permanent charges, not a distribution of potential. The binding sites and barriers of traditional

Concentration of ions along the channel

A

$[K^+]_i=[Cl^-]_i=100$mM, $\phi_{bi}(0)=23$mV
$[K^+]_o=[Cl^-]_o=1$mM, $\phi_{bi}(1)=137$mV
$V=100$mV, $P(z)=0.2$M

$[K^+]_o = 1\ mM$

Concentration of ions along the channel

B

$[K^+]_i=[Cl^-]_i=100$mM, $\phi_{bi}(0)=23$mV
$[K^+]_o=[Cl^-]_o=1$M, $\phi_{bi}(1)=3$mV
$V=100$mV, $P(z)=0.2$M

$[K^+]_o = 1\ M$

Potential Profile along the channel
$[K^+]_i=[Cl^-]_i=100$mM, $\phi_{bi}(0)=-23$mV
$P(z)=0.2$M, $V=100$mV

$[K^+]_o=[Cl^-]_i=1$mM
$\phi_{bi}(1)=137$mV
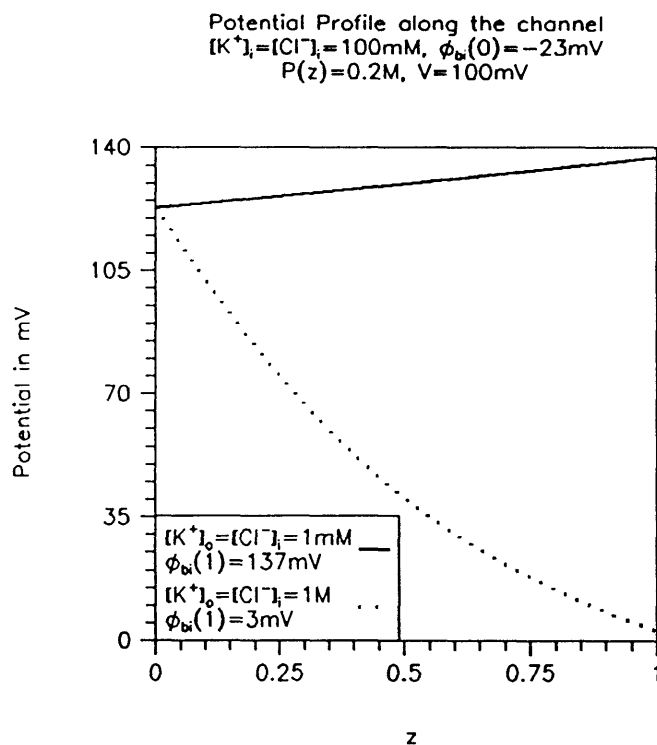$[K^+]_o=[Cl^-]_i=1$M
$\phi_{bi}(1)=3$mV

FIGURE 5 The profile of potential $\Phi(z)$ along a channel of uniform positive permanent charge with external concentrations of 1 mM and 1 M. Other parameters are described in text. The simplicity of the curves reflects the simplicity of the assumed structure of permanent charge. More complex structures produce much more complex behavior (7).
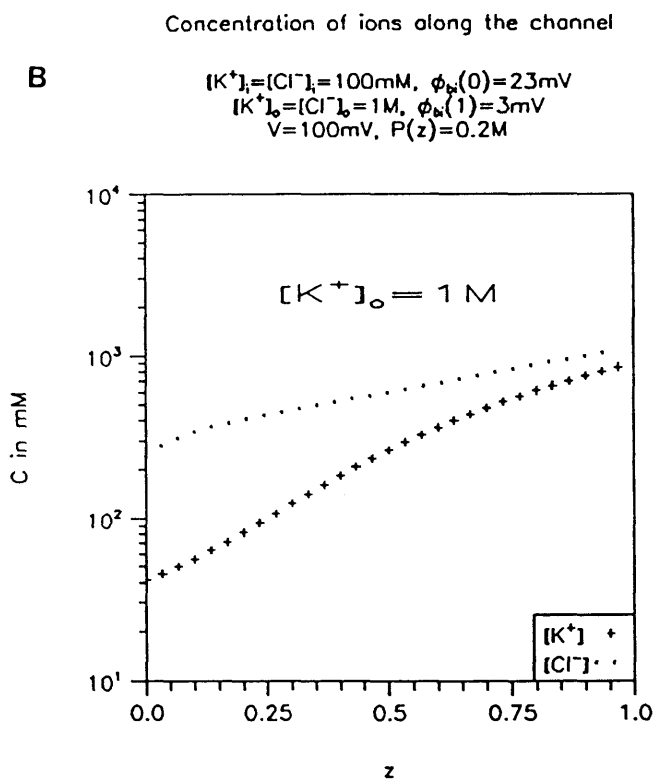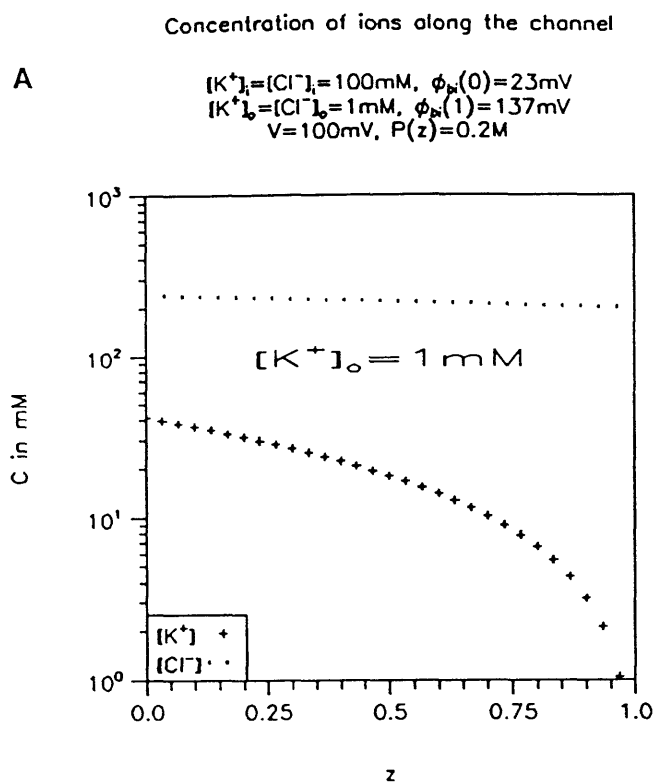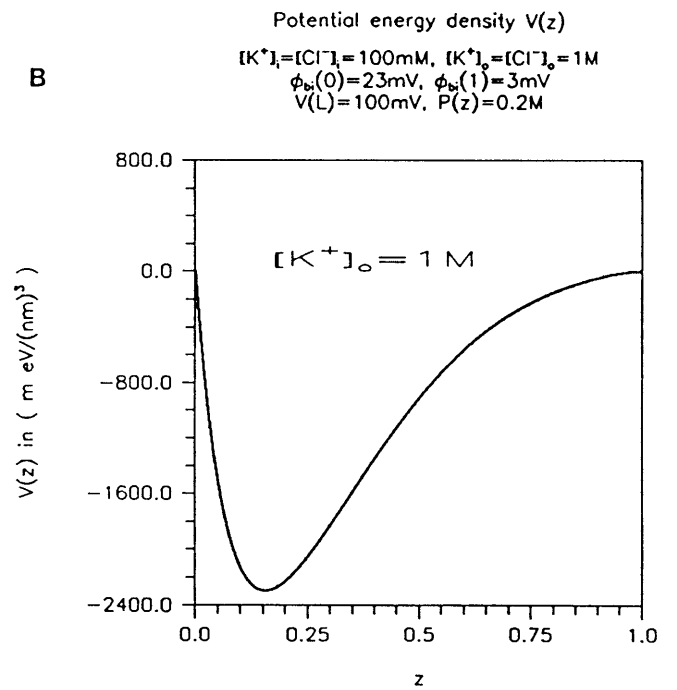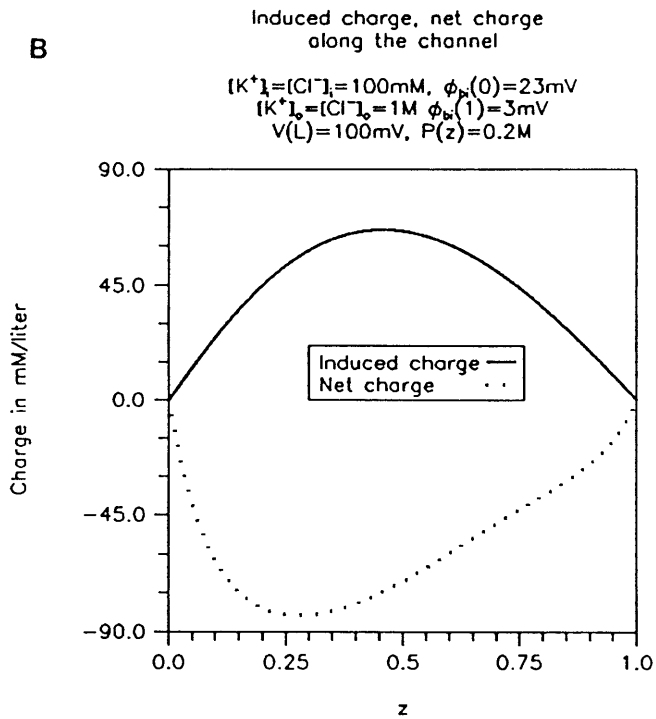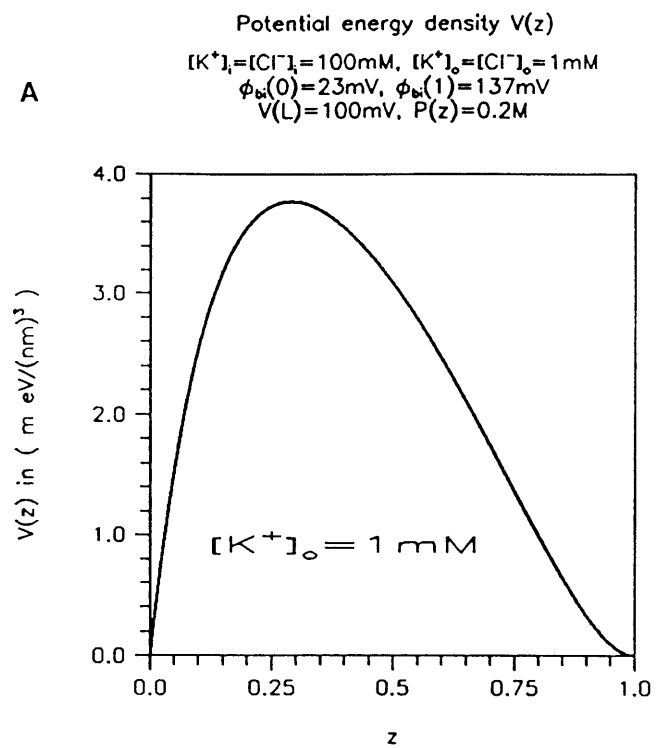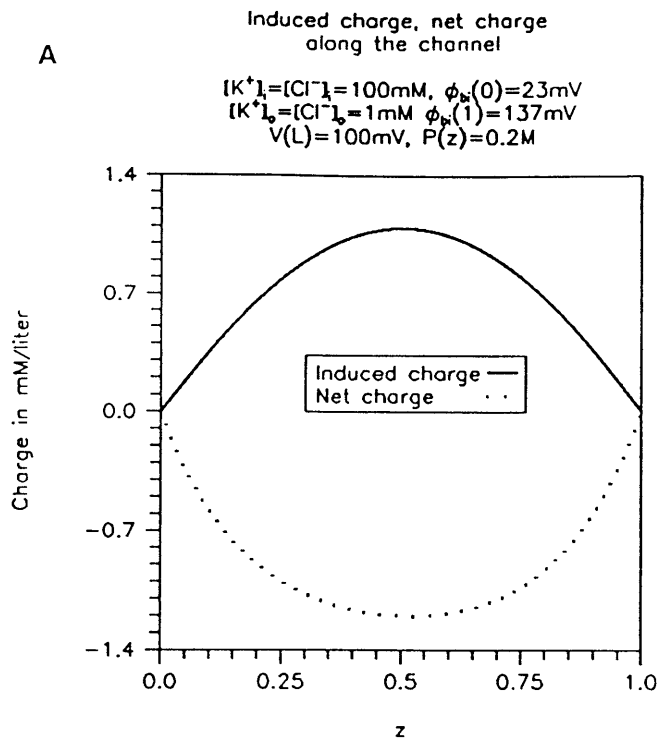
FIGURE 6 Concentration profile along a channel of uniform positive permanent charge with external concentrations of 1 mM (A) and 1 M (B). Other parameters are described in text. The simplicity of the curves reflects the simplicity of the assumed structure of permanent charge. More complex structures produce much more complex behavior (7).

A

Induced charge, net charge along the channel

$[K^+]_i=[Cl^-]_i=100mM$, $\phi_{bi}(0)=23mV$
$[K^+]_o=[Cl^-]_o=1mM$ $\phi_{bi}(1)=137mV$
$V(L)=100mV$, $P(z)=0.2M$

Charge in mM/liter

Induced charge ——
Net charge · ·

z

A

Potential energy density V(z)

$[K^+]_i=[Cl^-]_i=100mM$, $[K^+]_o=[Cl^-]_o=1mM$
$\phi_{bi}(0)=23mV$, $\phi_{bi}(1)=137mV$
$V(L)=100mV$, $P(z)=0.2M$

V(z) in (m eV/(nm)³)

$[K^+]_o= 1\ mM$

z

B

Induced charge, net charge along the channel

$[K^+]_i=[Cl^-]_i=100mM$, $\phi_{bi}(0)=23mV$
$[K^+]_o=[Cl^-]_o=1M$ $\phi_{bi}(1)=3mV$
$V(L)=100mV$, $P(z)=0.2M$

Charge in mM/liter

Induced charge ——
Net charge · ·

z

B

Potential energy density V(z)

$[K^+]_i=[Cl^-]_i=100mM$, $[K^+]_o=[Cl^-]_o=1M$
$\phi_{bi}(0)=23mV$, $\phi_{bi}(1)=3mV$
$V(L)=100mV$, $P(z)=0.2M$

V(z) in (m eV/(nm)³)

$[K^+]_o= 1\ M$

z

FIGURE 7.   Induced charge and net charge along a channel of uniform positive permanent charge with external concentrations of 1 mM (A) and 1 M (B). Other parameters are described in text. Note that the induced charge is quite significant when external concentration is 1 M, and the accompanying curves for net charge are quite different in that case.

FIGURE 8   The net potential energy density $V(z)$ of the charge stored in the channel of uniform positive permanent charge with external concentrations of 1 mM (A) and 1 M (B). Other parameters are described in text. The energy of binding of this concentration of ions depends dramatically in size and sign on the external concentrations: a barrier at low concentration becomes a well at a high concentration.

models come and go, as conditions change, as outputs of our calculations, not as assumptions of our theory.

DISCUSSION

Coupling

Some properties reminiscent of single filing and coupling are found in our results: e.g., efflux depending on *trans* concentration, and nonlinearity in conductance versus concentration. Others are not, most importantly the dependence of the flux ratio on concentration and potential gradient. But our analysis of the two-ion case of the PNP theory does not include selectivity and does not reproduce the usual physiological situation (however, see references 41, 46, and 47), where (at least) three ions are varied to adjust concentration while maintaining ionic strength.

Macro- and microscopic parameters

The parameters and variables of this theory are macroscopic averages of the underlying microscopic stochastic variables, and the relation of the averages and the underlying probability functions is different for each parameter and variable. In particular, the variables of our theory lump together stochastic processes that may occur at different times: macroscopic averages overlap in time even when the underlying microscopic processes do not. For example, the macroscopic "concentration in a pore" might include several different (types of) ions when microscopically the pore is occupied by only one (type of) ion at a time. In this situation, macroscopic concentration would depend on the occupancy of the pore (i.e., fraction of time occupied by a particular number and/or type of ion) as much as on the number of ions that fit in the pore.

Occupancy, structure, permanent charge, and the built-in potential

The macroscopic free charge density $\tilde{q}(z) = (\lambda^2/I_c) \times \sum z_j C_j(z)$ of Eqs. A2, 2, and 3 ought to depend on occupancy because the concentrations of each ion $C_j(z)$ depend on the occupancy of the channel, as just described. Each concentration $C_j(z)$ is, almost certainly, proportional to both the fraction of the time that ion is in the channel and to the number of ions (of that type) in the channel when it is occupied. The net space charge $\tilde{q}(z)$ ought to depend linearly on occupancy time of each ion, and variables that depend on the space charge (like the built-in potential) will reflect this linear dependence. Note that dependence on total occupancy time (i.e., the sum of occupancy times of each ion) may be much more complex than dependence on occupancy time of single types of ions.

The macroscopic variable–induced charge σ_{pol} (Eqs. 2, A21, and A25) also ought to depend on occupancy,

but in a more complex way. One component of induced charge $2\tilde{\epsilon}(1 - z)\Delta$, namely, that produced by just the transmembrane potential, ought to be independent of occupancy time if the (average) transmembrane potential is independent of time, on a microscopic time scale. The other component of induced charge, $2\tilde{\epsilon}\Phi(z)$ of Eq. 2, produced by the ion in the pore, ought to depend on occupancy because it is present only when the channel is occupied. That component $2\tilde{\epsilon}\Phi(z)$ does in fact depend on occupancy because the potential $\Phi(z)$ depends on $C_j(z)$, which itself depends on occupancy, as we have seen.

The macroscopic permanent charge density $P(z)$ seems at first to be a microscopic variable independent of occupancy in both cases. This would indeed be the case of the structure of the channel were constant, independent of the chemical nature of the ion in the channel. But the average structure does depend on occupancy, and so the macroscopic variable $P(z)$ must depend on occupancy, because a protein channel is anything but rigid. The channel protein gramicidin (48) is known to adopt different conformations when occupied by different ions; permeation of different ions may occur through channels of different conformations: permeation resembles a snake swallowing a rabbit rather than a pipe channeling a ball (49). Thus, we must remember that permanent charge $P(z)$ in a model like ours represents the conformation of charges within the channel protein while an ion is permeating the channel pore.

The dependence of structure on occupancy is to be expected for another reason, because different ions follow different paths as they permeate a channel. Different ions permeating crystalline channels fit differently into the periodic structure of the crystal and thus interact with different distributions of permanent charge, when viewed in the coordinates of the permeating ion: commensurate (i.e., good) fits produce higher barriers and lower conductance; incommensurate (i.e., bad) fits produce lower barriers and higher conductance (50). (Roux and Karplus [51, p. 974-975: Fig. 16] find similar phenomena in simulations of gramicidin using boundary conditions periodic at all times in all the coordinates of phase space, namely, both the velocity and position of every atom. Such boundary conditions are likely to produce a much more rigid structure than any protein, let alone crystal, where, after all, only the mean atomic position is periodic, and the thermal fluctuations in those positions are substantial.) An ion that fits well into a channel fits comfortably into a potential well, sitting near its bottom, far from the potential maximum. It needs to climb a large barrier to escape. An ion that fits poorly sits nearer the top of the potential well, nearer the potential maximum. It needs to climb a smaller barrier to escape. The present model would need one arrangement of permanent charge to describe a well-fitting ion and another to describe an ill-fitting ion: each ion j would be in a different radial position, each would follow

a different reaction path, and each would interact with a different effective permanent charge $P_j(z)$.

Any parameter that depends on structure ought then to depend on occupancy, viz., the diffusion coefficient $D_j(z)$; the dielectric coefficients $\varepsilon_{r1}(z)$ and $\varepsilon_{r2}(z)$ of the aqueous medium and channel protein; perhaps even the length d and radius a of the pore. Most significantly, the built-in potential ought to depend on occupancy and be different for each type of ion. The built-in potential is in series with the pore and thus all parameters of (charge) transport should depend on occupancy.

Although this verbal discussion of occupancy seems correct, we are more than aware that a stochastic version of the dielectric theory, analytical or numerical, is needed to give precise physical meaning and (we hope) mathematical support to our conclusions, particularly because the overall system is so nonlinear. Without such support, discrepancies should be expected when comparing the charge densities of the model with charge densities estimated in actual channel proteins.

Built-in potential

The built-in potential in our model of a single open channel is expected to behave in some ways like the Donnan potential (4) or "surface potential" used for many years in the description of currents in macroscopic measurements (both the "instantaneous" currents of the open channel and the evolving currents reflecting channel gating). Frankenhaeuser and Hodgkin (52; as suggested by A. F. Huxley) explained the effects of Ca^{2+} (chiefly on gating) and the effects of $[Na^+]$ (chiefly on the shape of the instantaneous current–voltage curve) by shifts of the surface potential. Shifts in surface potential have been used extensively ever since (6, 53) to explain the horizontal shifts in the plot of "something" versus potential produced by many experimental interventions, most notably pharmacological agents. Typically, "something" ≡ some measure of activation or voltage dependence, originally the Hodgkin–Huxley (54) variables m and h. To fit their macroscopic data, involving many channels and gating phenomena, Hodgkin and Frankenhaeuser (see p. 161 of Frankenhaeuser [55]) postulate a surface potential that varied (just) Na^+ concentration at the outside mouth of the pore. We will return to this postulate in another paper. Chandler and Hodgkin (41) presented a theory of the built-in potential (at the inside mouth of the pore) not very different from that presented here and used it to describe and explain macroscopic currents measured with (internal) solutions of varying ionic strength, currents that depend on the number of channels open (i.e., gating) as well as the properties of the open channel (46, 47). We hope to return again to these macroscopic data, if we are able to further extend the PNP theory (7) to describe time-dependent properties of individual channels (e.g., flickering, opening, or closing between full or subconductance states) and their ensembles (e.g., gating).

Shifts in potential dependence would also, of course, be produced by permanent charge in antechambers to the pore (56, 57), or other structures like basement membranes, not included in our model. More refined versions of our permanent charge model could describe antechambers as a part of the pore with distinct parameters for each ion, e.g., diameter, permanent charge density, and diffusion coefficients.

It is not always realized that shifts along the potential axis might also be produced by charges in the membrane away from the pore, structures that are in parallel with the pore, and charges not in the pathway for ionic movement. The PNP theory (2, 3) shows that such potentials "switch back" (i.e., spread) from the far field away from the pore into the near field within the pore, essentially because the potential across the pore/protein interface $r = a$ is continuous at each z, i.e., $\phi(z, a, \theta) = \Psi(z, a, \theta)$ (Eq. A31). An offset in the far-field potential might be produced by surface charge in the channel protein (away from the pore), surface charge in neighboring lipid, or surface charge in adjacent accessory proteins (such as receptors). All would change the potential within the pore. Binding of agonists to such a receptor would change the parallel surface charge, modifying the far field and thus the potential in the pore. That potential would change the current through the pore, if it were already open. It might activate and open a channel, if it were initially closed, by switching it from one current–voltage relation to another, that is to say, from one solution of the Eqs. 2, 5, and 11–13 to another (7).

Distribution of charge

This paper describes an oversimplified model of a channel of one conformation in the presence of just two types of ions, described as points. Nonetheless, interesting effects reminiscent of coupling are found as solutions are changed. These effects occur because the distribution of potential and potential energy is not (indeed, cannot be) constant when bathing solutions are changed. Coupling in this model reflects changes in the spatial distribution of free charge, potential, and potential energy, in contrast to traditional paradigms in which coupling reflects changes in the shape (i.e., conformation) of the protein, i.e., movement of its atoms and (thus) change in the distribution of permanent charge $P(z)$. In our model, the conformation of the protein is defined as $P(z)$, the distribution of permanent charge. This conformation is held constant in our analysis, while the spatial distributions of mobile charge, potential, and potential energy vary, in response to changes in solutions and conditions, as determined by the PNP theory.

The spatial arrangements of free and induced charge in the present model arise as the output of the PNP theory, the solution of a system of nonlinear differential equations. As such, these distributions of charge cannot be predicted by physical reasoning before the calculations reveal them, at least by the present authors, al-

though physical reasoning easily explains the conformations after the calculations are made. In traditional models, conformations (i.e., states) are inputs to the model, vaguely defined in terms of the structure of the protein, created to describe the coupling of fluxes observed in experiments, and little else: conformations are rarely measured experimentally and are not outputs, derived theoretically, as far as we are aware, in traditional work.

The next paper in this series will describe a channel bathed in solutions with more than two ions, a channel containing a selectivity filter and one (spatially nonuniform) conformation of permanent charge. As we write, we do not known what subset of biological phenomena can be described by such models: further analysis and conformation with data will tell that. If a simple model of one state (i.e., conformation of permanent charge) can account for experimental data, it is preferable, at least in our view, to a complex model that introduces many states to fit a particular data set, even if the states describe the occupancy in a stochastic model. But a rigid model of one conformation is not likely to fit all experimental conditions and data sets: after all, proteins are not rigid molecules. Proteins can and do change shape, and state models describing transitions between conformations are one way to describe such flexibility.

State models must describe each conformation of the protein as an arrangement of permanent charge, not a distribution of potential,[5] if the conformation is supposed to be independent of experimental conditions (i.e., ionic concentration): conservation of charge implies that the distribution of potential within the protein varies as experimental conditions vary, even if (or should we say, just because) the distribution of permanent charge does not. Furthermore, each state (and each mechanism allowing change in state) should be related to the physical parameters that must characterize any protein, e.g., size (e.g., length and diameter), dielectric coefficient, distribution of permanent charge, composition of bathing solutions, and so on. Only in this way can state models can be specific, falsifiable, and thus experimentally useful.

APPENDIX

Derivation

Poisson's equation describes how the electrostatic field $E(x, R, \theta)$ depends on charge $\rho(x, R, \theta)$ (units: C/m^3) of all types:

$$\epsilon_0 \nabla \cdot E(x, R, \theta) = \rho(x, R, \theta), \quad (A1)$$

where ϵ_0 is the proportionality coefficient between electric field and charge in a vacuum, the permittivity of empty space, some 8.85 pF/m; (x, R, θ) are cylindrical coordinates (units: m, m, rad) and

---

[5] Although more than one distribution of potential can arise from one conformation of permanent charge (7, 42–44).

$$\rho(x, R, \theta) = \overbrace{P(x, R, \theta)}^{\substack{\text{Permanent} \\ \text{charge}}} + \overbrace{\rho_i(E; \Delta; x, R, \theta)}^{\substack{\text{Induced} \\ \text{charge}}}$$

$$+ \overbrace{q(E[\tilde{x}, \tilde{R}, \tilde{\theta}]; x, R, \theta)}^{\substack{\text{Ionic, mobile, space} \\ \text{charge}}}. \quad (A2)$$

We use the language of vector calculus invented (58–60) to describe such fields.

Charge in electrolyte solutions

Equations like A1 can sometimes mislead, because they describe only part of the interactions of charge and field. They describe how the field depends on its source, the charge distribution, but not how the source, the charge distribution, depends on the field. The existence of two kinds of charge, that induced by the field (zero when the field is zero), and that independent of the field (present even when the field is zero), caused much difficulty to early investigators of electromagnetism (according to historical analyses [26–29]; Buchwald [28] traces the development of the modern theory involving both permanent and induced charge). Modern texts still do not make the distinction clearly when describing boundary conditions, particularly those involving permanent charge and junctions between dielectrics.

In the present context, three types of charge are important and each depends on the electric field in a different way, shown by the awkwardly explicit notation for the arguments.

The permanent charge $P(x, R, \theta)$ (units: C/m^2) depends only on position. It is the Schrödinger equation's unperturbed distribution of protons and electrons in the atoms and chemical bonds of the channel protein, the electron distribution measured by, for example, x-ray crystallography (Ch. 6 of Creighton [61]; p. 94 et seq. of Cowley [62]). From the point of view of both ion permeation and x-ray crystallography, $P(x, R, \theta)$ is the structure of the channel. The field determined by this charge can be computed by a multipole expansion (Panofsky and Phillips [23], p. 17, et seq.; Stratton [63], p. 172 et seq.), if one insists on following tradition, writing the electric field as the sum of fields arising from a monopole, dipole, quadrupole, etc. However, almost all biological interactions occur close to a molecule, and, there, close to the charge distribution, the multipole expansion is a "fruitless exercise" (Purcell [22], p. 355) because it requires many (hundreds or thousands of) terms, decreasing in magnitude as $1/n$ (e.g., Olver [34]), to decently approximate the electric field of the molecule. We deal directly with the entire distribution of charge, which includes, of course, all the effects of dipoles, quadrupoles, etc.

The induced charge $\rho_i(E; \Delta; x, R, \theta)$ depends on position, the electric field at that position, and the transmembrane potential Δ (in our problem). It does not exist when the electric field is zero.[6] The induced charge is sometimes confusingly called "fixed" or "bound" charge, but induced charge is fixed or bound only in the sense that it is not free to move macroscopic distances. Induced charge is flexibly bound in molecules, free to move or orient only tiny distances, conceivably moving as a unit with characteristic time and voltage dependence.

The ionic or free charge in the channel's pore $q(E[\tilde{x}, \tilde{R}, \tilde{\theta}]; x, R, \theta)$ forms a space charge density that depends on location and on the electric field at all other locations $[\tilde{x}, \tilde{R}, \tilde{\theta}]$ as well, because it is free to move macroscopic distances, indeed, to leave the system (i.e., pore) altogether. The volume density of such charge, in somewhat simplified notation, is

$$q(x, R, \theta) = \sum_j e z_j c_j(x, R, \theta). \quad (A3)$$

---

[6] $\rho_i(E; \Delta; x, R, \theta)$ is not named "polarization" because that word might be misunderstood to include dipolar charge that exists when E = 0. Also, the scalar $\rho_i(E; \Delta; x, R, \theta)$ should not be given the same name as the vector $P(E; \Delta; x, R, \theta)$, the polarization of Eq. 13.

Such ions carry flux J_j (units: $m^{-2} \cdot sec^{-1}$) through macroscopic distances, driven by diffusion and electric fields according to the Nernst–Planck equations, written, in somewhat simplified notation,

$$J_j(x, \text{R}, \theta) = D_j$$

$$\times \left\{ -\nabla c_j(x, \text{R}, \theta) + \frac{z_j e}{kT} c_j(x, \text{R}, \theta) \cdot E(x, \text{R}, \theta) \right\} . \quad (A4)$$

The independent variables, e.g., the electric field $E(x, \text{R}, \theta)$, flux $J_j(x, \text{R}, \theta)$, and concentration $c_j(x, \text{R}, \theta)$ (units: number/m^3) generally depend on all the other variables at all locations, on the transmembrane potential, and on all the other parameters of the problem. The flux of each ion also depends on many parameters. It is stationary on the biological time scale and satisfies the conservation law, the continuity equation

$$\nabla \cdot J_j(x, \text{R}, \theta) = 0. \quad (A5)$$

z_j is the charge on each ion, positive for cations, negative for anions in units of e, the charge on the proton, 1.6×10^{-19} C; k is Boltzmann's constant and T is the absolute temperature; $D_j(x)$ is the diffusion coefficient (m^2/s) of the jth ion in the channel pore and is allowed to depend on location. This diffusion coefficient is inversely proportional to the friction on an ion moving in the pore. That friction may be very different from the friction in bulk solution, because the environment of an ion in a pore is very different from the environment in free solution. The selectivity of channels might arise from differences in D_j among ions, as in classical constant-field theory, where different ions are assumed to have different frictional interactions with the channel protein.

The potential $\varphi(x, \text{R}, \theta)$ (units: volts) is defined implicitly by

$$-\nabla \varphi(x, \text{R}, \theta) \equiv E(x, \text{R}, \theta) \quad (A6)$$

along with sign conventions. Imagine a channel placed horizontally across a vertical membrane. The potential on the left-hand side of a channel corresponds to the inside of the membrane or cell and is assumed to be $\varphi(x = 0) = V$, where we also choose the origin of the longitudinal coordinate x; d is the channel length. The potential on the right-hand side, the outside of the cell or membrane, is assumed zero, $\varphi(x = d) = 0$, positive flux and current is taken to be outward (from left to right). These conventions preserve the usual sign conventions of membrane physiology (following Hodgkin [64]), Ohm's law (in the absence of concentration gradients), Fick's law (in the absence of electrical gradients), and the derivative, as the limit of a forward difference.

We write the equations generally for future reference, although only two ions are considered in this paper. The concentration of each ion $c_j(x = 0)$ (units: $1/m^3$) is described by its fraction l_j of the total concentration c_L on the left-hand side

$$c_j(x = 0) = l_j \cdot c_L; \quad l_j = \frac{c_j(x = 0)}{\sum\limits_{z_j > 0} c_j z_j} \quad (A7)$$

or its fraction r_j of the total concentration c_R on the right-hand side:

$$c_j(x = d) = r_j \cdot c_R; \quad r_j = \frac{c_j(x = d)}{\sum\limits_{z_j > 0} c_j z_j} . \quad (A8)$$

We revert to more traditional physiological notation soon.

Boundary conditions are needed to complete the specification of the problem and, as usual, are of the greatest importance. Electrical neutrality is assumed in each bath, far away from the channel (but not close to the channel or within the pore), so on the left-hand side

$$\sum\limits_{z_j > 0} l_j z_j = -\sum\limits_{z_j < 0} l_j z_j = 1 \quad \text{at} \quad x = -\infty \quad (A9)$$

and on the right-hand side

$$\sum\limits_{z_j > 0} r_j z_j = -\sum\limits_{z_j < 0} r_j z_j = 1 \quad \text{at} \quad x = +\infty. \quad (A10)$$

Ions are confined to the pore by forbidding radial flux at the wall of the channel $r = a$,

$$J_j \cdot \mathbf{r} = \frac{\partial c_j(a, x)}{\partial r} + \frac{z_j e}{kT} \cdot c_j(a, x) \cdot \frac{\partial \varphi(a, x)}{\partial r} = 0, \quad (A11)$$

where $\mathbf{r}$ is the radial unit vector. But boundary conditions do not prohibit longitudinal flux or current flow in or out of the mouth of the channel: mobile ions are free to come and go.

The potential within the pore is linked to the potential within the surrounding channel protein by dielectric boundary conditions derived in the text, after Eq. 9.

The experimental variable measured in most single channel experiments is the current $I(V)$ flowing out of the channel mouth, the spatial integral of the fluxes

$$I(V) = \sum\limits_j 2\pi e z_j \int_0^a J_j(r, d) \cdot \mathbf{r} r \, dr. \quad (A12)$$

To use these equations, we must describe the types, locations, and properties of charge in the channel and its pore.

Induced charge

The induced charge $\rho_i(E; \Delta; x, \text{R}, \theta)$ (units C/m^3) moves just a few angstroms in the electric field, making a surplus in one location that balances a deficit elsewhere, creating tiny charge dipoles that sum to zero total charge, described by the volume density of dipoles, the polarization field $P(E; x, \text{R}, \theta)$, with units coulomb $\times$ meter/[meter]^3 = C/m^2, defined implicitly by

$$-\nabla \cdot P(E; x, \text{R}, \theta) \equiv \rho_i(E; \Delta; x, \text{R}, \theta) \quad (A13)$$

with the minus sign appearing because induced dipoles point in the opposite direction from $E(x, \text{R}, \theta)$. The polarization measures the movement and amount of charge induced by an electric field: it is a measure of the flexibility of the molecular structure, e.g., the movement of the channel protein in response to a particular electric field.

Now, consider the common case where the polarization $P(E; x, \text{R}, \theta)$ depends only on the local electric field $E(x, \text{R}, \theta)$ and that in the simplest possible way, namely, proportionately:

$$P(E; x, \text{R}, \theta) = \chi \epsilon_0 E(x, \text{R}, \theta) = (\epsilon - \epsilon_0) E(x, \text{R}, \theta)$$

$$= (\epsilon_r - 1) \epsilon_0 E(x, \text{R}, \theta). \quad (A14)$$

χ is the proportionality coefficient between field and polarization, the susceptibility (dimensionless); ϵ is the proportionality coefficient between field and charge, the permittivity (units: farad/m); ϵ_r is that permittivity compared to free space (dimensionless), the relative permittivity or, more informally, the dielectric coefficient:

$$\epsilon_r \equiv \frac{\epsilon}{\epsilon_0} = 1 + \chi. \quad (A15)$$

These parameters all measure how much and how far charge moves per unit field when an electric field is applied to a protein: they measure the flexibility of each charged structure in the protein. Writing each parameter as a single real number is equivalent to assuming that every charged structure moves on a much faster time scale than the biological phenomena of interest, reaching a stationary displacement, proportional to the local electric field strength, much faster than ions permeate channels.

It is possible to define a new field $D(x, \text{R}, \theta)$ that describes a linear combination of the electric and polarization fields, following Maxwell's

approach. Using Eqs. A13–A15 to describe the induced charge $\rho_i(x, R, \theta)$ in Eqs. A1 and A2 gives

$$\nabla \cdot [\epsilon_0(1 + \chi)E(x, R, \theta)] = \nabla \cdot [\epsilon E(x, R, \theta)]$$
$$= P(x, R, \theta) + q(x, R, \theta). \quad (A16)$$

So it is natural to define a new field $D(P; E; x, R, \theta)$ and write

$$\epsilon_0(1 + \chi)E(x, R, \theta) \equiv D(P; E; x, R, \theta) = \epsilon E(x, R, \theta)$$
$$= \epsilon_0 E(x, R, \theta) + P(E; x, R, \theta), \quad (A17)$$

giving the traditional (since Heaviside [65], 1886, reprinted 1970) and then Hertz: Hunt [33], p. 122–128; Nahin [66], p. 108–110) textbook result,

$$\nabla \cdot D(x, R, \theta) = P(x, R, \theta) + q(x, R, \theta), \quad (A18)$$

in addition to the more explicit formulation of Eqs. A1 and A2 favored by modern workers (Ch. 10 of Purcell [22]; Ch. 10 of Feynmann [67]). Eq. A17 combines the electric field with the polarization field, which depends linearly and locally on it. Eq. A18 treats permanent and (the nonlinear nonlocal) space charge of mobile ions as the source for the D field. Eqs. A1 and A2 treat all charges on an equal footing as equivalent sources of the E field.

Note that if the dielectric properties of the material vary with location, Eq. A18 does not change but Eq. A16 becomes

$$\nabla \cdot (\epsilon E) \equiv \epsilon \nabla \cdot E(x, R, \theta] + (\nabla \epsilon) \cdot E(x, R, \theta)$$
$$= P(x, R, \theta) + q(x, R, \theta) \quad (A19)$$

or

$$\epsilon \nabla \cdot E(x, R, \theta)$$
$$= P(x, R, \theta) + q(x, R, \theta) - (\nabla \epsilon) \cdot E(x, R, \theta). \quad (A20)$$

Thus, the spatial variation of dielectric properties, in particular the gradient $\nabla \epsilon$ of the dielectric permittivity, helps form a source of the electric field $E(x, R, \theta)$ but not the displacement field $D(x, R, \theta)$.

Boundary conditions at the channel's wall

Charges at the boundary between the aqueous pore and the channel wall are sources of the electric field $E(x, R, \theta)$ just as significant as the volume charge q within the pore.

Permanent surface charge $\sigma_0(x) = P(x, R, \theta) \cdot (\pi a^2 \cdot d/2\pi a \cdot d)$ at the boundary, where a is the channel radius, is independent of $E(x, R, \theta)$ or $c_j(x, R, \theta)$ but can vary with x. Induced surface charge at the boundary, but in region 1, the pore, is called $\sigma_1(E, x)$; induced charge at the boundary, but in region 2, the channel protein, is called $\sigma_2(E, x)$. The total induced charge is the polarization charge:

$$\sigma_{pol}(E; x) \equiv \sigma_2(E, x) - \sigma_1(E, x). \quad (A21)$$

Boundary conditions at a junction of dielectrics of relative permittivities $\epsilon_{r1}(x)$ and $\epsilon_{r2}(x)$ can be derived from the standard pillbox construction and analysis (e.g., Panofsky and Phillips [23], p. 31–32: a reference that helpfully uses SI units) once the properties of the charge at the boundary are specified by a physical model.

Our view of the boundary between channel protein and pore retains the surface charges $\sigma_0(x)$, $\sigma_1(x)$, and $\sigma_2(x)$ (units: C/m^2) within the pillbox, even as its thickness shrinks to zero, in contrast to the volume charge $q(x, R, \theta) = \sum ez_j c_j(x, R, \theta)$ (units: C/m^3) of ions which tends to zero as the thickness shrinks. Then, Eq. A18 gives

$$\hat{n} \cdot (D_2 - D_1) = \sigma_0(x). \quad (A22)$$

A pillbox treatment starting from Eqs. A1 and A2 gives the equivalent

$$\hat{n} \cdot (E_2 - E_1) = \frac{\sigma_0(x) - \sigma_1(E; x) + \sigma_2(E; x)}{\epsilon_0}. \quad (A23)$$

Corresponding boundary conditions can be written for the potential, using Eq. A20 to handle dielectric properties that vary along the boundary. $\psi(x, a, \theta)$ is the potential just outside the boundary in the channel protein and $\varphi(x, a, \theta)$ is the potential just inside the boundary in the pore.

$$\varepsilon_{r2}(x) \cdot \frac{\partial \psi}{\partial R}(x, a) - \varepsilon_{r1}(x) \cdot \frac{\partial \varphi}{\partial R}(x, a) = -\frac{\sigma_0(x)}{\epsilon_0} \quad (A24)$$

From Eqs. (A1) and (A2),

$$\frac{\partial \psi}{\partial R}(x, a) - \frac{\partial \varphi}{\partial R}(x, a)$$

$$= -\underbrace{\frac{\sigma_0(x)}{\epsilon_0}}_{\substack{\text{Permanent} \\ \text{charge}}} - \underbrace{\frac{\sigma_2(E, x) - \sigma_1(E, x)}{\epsilon_0}}_{\substack{\text{Induced} \\ \text{charge}}}. \quad (A25)$$

Note the alternative descriptions of the induced charge, the dielectric fcoefficient in Eq. A24, and induced charge density in Eq. A25. These descriptions can be mixed, if desired, for example, by replacing either induced surface charge density with its equivalent dielectric representation, e.g.,

$$\sigma_1(E, x) = (\epsilon_1 - \epsilon_0)E_1 \cdot \hat{n} = (\epsilon_1 - \epsilon_0)\frac{\partial \varphi}{\partial R}(x, a)$$

$$= (\varepsilon_{r1} - 1)\epsilon_0 \frac{\partial \varphi}{\partial R}(x, a)$$

$$\sigma_2(E, x) = (\epsilon_2 - \epsilon_0)E_2 \cdot \hat{n} = (\epsilon_2 - \epsilon_0)\frac{\partial \psi}{\partial R}(x, a)$$

$$= (\varepsilon_{r2} - 1)\epsilon_0 \frac{\partial \psi}{\partial R}(x, a). \quad (A26)$$

Now it is time to introduce dimensionless units

$$\phi = \varphi e/kT \quad \Psi = \psi e/kT \quad r = R/a \quad z = x/d$$
$$\alpha = a/d \quad \varepsilon = \epsilon_2/\epsilon_1 = \varepsilon_{r2}/\varepsilon_{r1}, \quad (A27)$$

where the length of the channel is d and its radius a. The nondimensional permanent surface charge $\omega_0(z)$ is

$$\omega_0(z) = \frac{e}{kT} \cdot \frac{a}{\varepsilon_{r1}} \frac{\sigma_0}{\epsilon_0} = \frac{e}{kT} \cdot \frac{a^2}{2\varepsilon_{r1}\epsilon_0} P(x, R, \theta). \quad (A28)$$

The dielectric boundary conditions become

$$\frac{\partial \phi}{\partial r}(z, a) = \epsilon(z) \cdot \frac{\partial \Psi}{\partial r}(z, a) + \omega_0(z). \quad (A29)$$

The surface charge boundary condition is (cf. Eq. A26)

$$\frac{\partial \phi}{\partial r}(z, a)$$

$$= \frac{\partial \Psi}{\partial r}(z, a) + \frac{ea}{kT}\frac{\sigma_0 - \sigma_1(E, z) + \sigma_2(E, z)}{\epsilon_0} \quad (A30)$$

and the continuity of potential at an interface of dielectrics is

$$\phi(z, a, \theta) = \Psi(z, a, \theta). \qquad (A31)$$

In this description of the boundary $r = a$, the charges of a dipole embedded in the interface (frequently discussed in electrode theory [36, 68]) must be allocated to one medium or the other.

REFERENCES

1. Chen, D. P., V. Barcilon, and R. S. Eisenberg. 1992. Constant field and constant gradients in open ionic channels. *Biophys. J.* 61:1372–1393.

2. Barcilon, V. 1992. Ion flow through narrow membrane channels. Part 1. *SIAM (Soc. Ind. Appl. Math.)-SIMS (SIAM Inst. Math. Soc.) Conf. Ser.* 52:1391–1404.

3. Barcilon, V., D. P. Chen, and R. S. Eisenberg. 1992. Ion flow through narrow membranes channels. Part II. *SIAM (Soc. Ind. Appl. Math.)-SIMS(SIAM Inst. Math. Soc.) Conf. Ser.* 52:1405–1425.

4. Teorell, T. 1953. Transport processes and electrical phenomena in ionic membranes. *Prog. Biophys. Mol. Biol.* 3:305–369.

5. Hodgkin, A. L., and B. Katz. 1949. The effect of sodium ions on the electrical activity of the giant axon of the squid. *J. Physiol. (Lond.).* 108:37–77.

6. Hille, B. 1992. Ionic Channels of Excitable Membranes. 2nd ed. Sinauer Associates, Inc., Sunderland, MA. 607 pp.

7. Chen, D. P., and R. S. Eisenberg 1992. Electric fields in biological channels. *J. Gen. Physiol.* 100:9a. (Abstr.)

8. Jacobs, M. H. 1935. Diffusion Processes. Springer Verlag, New York. 160 pp.

9. Hille, B. 1989. Transport across cell membranes: carrier mechanisms. *In* Textbook of Physiology. Vol. 1. 21st ed. H. D. Patton, A. F. Fuchs, B. Hille, A. M. Scher, and R. D. Steiner, editors. W. B. Saunders Co., Philadelphia, PA. 24–47.

10. Hodgkin, A. L. 1951. The ionic basis of electrical activity in nerve and muscle. *Biol. Rev.* 26:339–409.

11. Sten-Knudsen, O. 1978. Passive transport processes. *In* Membrane Transport in Biology: Concepts and Models. Vol. 1. D. C. Tosteson, editor. Springer-Verlag, New York. 5–113.

12. Bass, L., and A. J. Bracken. 1983. The flux-ratio equation under nonstationary boundary conditions. *Math. Biosci.* 66:87–92.

13. Bass, L., and A. McNabb. 1988. Flux ratio theorems for nonlinear membrane transport under nonstationary conditions. *J. Theor. Biol.* 133:185–191.

14. Hodgkin, A. L., and R. D. Keynes. 1955. The potassium permeability of a giant nerve fibre. *J. Physiol. (Lond.).* 128:61–88.

15. Hodgkin, A. L., and R. D. Keynes. 1955. Active transport of cations in giant axons from *Sepia* and *Loligo. J. Physiol. (Lond.).* 128:28–60.

16. Shaw, T. I. 1955. Potassium movements in washed erythrocytes. *J. Physiol. (Lond.)* 129:464–475.

17. Glynn, I. M. 1956. Sodium and potassium movements in human red cells. *J. Physiol. (Lond.).* 134:278–310.

18. Gunn, R. B., and O. Fröhlich. 1979. Asymmetry in the mechanism for anion exchange in human red blood cell membranes: evidence for reciprocating sites that react with one transported anion at a time. *J. Gen. Physiol.* 74:351–374.

19. Forbush, B. 1987. Rapid release of ^{45}K and ^{86}Rb from an occluded state of the Na,K-pump in the presence of ATP or ADP. *J. Biol. Chem.* 262:11104–11115.

20. Forbush, B. 1987. Rapid release of ^{42}K or ^{86}Rb from two distinct transport sites on the Na,K-pump in the presence of P_i or vanadate. *J. Biol. Chem.* 262:11116–11127.

21. Glynn, I. M., and S. J. D. Karlish. 1990. Occluded cations in active transport. *Annu. Rev. Biochem.* 59:171–205.

22. Purcell, E. M. 1985. Electricity and Magnetism: Berkeley Physics Course. Vol. 2. 2nd ed. McGraw-Hill Book Co., New York. 484 pp.

23. Panofsky, W. and M. Phillips. 1962. Classical Electricity and Magnetism. 2nd ed. Addison Wesley Publishing Co., New York. 494 pp.

24. Jackson, J. D. 1975. Classical Electrodynamics. 2nd ed. John Wiley & Sons, New York. 848 pp.

25. Scott, W. T. 1959. The Physics of Electricity and Magnetism. John Wiley & Sons, New York. 635 pp.

26. Siegel, D. M. 1991. Innovation in Maxwell's Electromagnetic Theory. Cambridge University Press, New York. 225 pp.

27. Hendry, J. 1986. James Clerk Maxwell and the Theory of the Electromagnetic Field. Adam Hilger Ltd., Boston. 305 pp.

28. Buchwald, J. D. 1985. From Maxwell to Microphysics. The University of Chicago Press, Chicago, IL. 339 pp.

29. Hunt, B. J. 1991. The Maxwellians. Cornell University Press, New York. 266 pp.

30. Deb, B. M. 1981. The Force Concept in Chemistry. Van Nostrand Reinhold, New York. 502 pp.

31. Böttcher, C. J. F. 1973. Theory of Electric Polarization. Elsevier Scientific Publishing Co. Inc., New York. 377 pp.

32. Eringen, A. C. and G. A. Maugin. 1990. Electrodynamics of Continua. II. Fluids and Complex Media. Springer Verlag, New York. 368 pp.

33. Kevorkian, J., and J. D. Cole. 1981. Perturbation Methods in Applied Mathematics. Springer-Verlag, New York. 558 pp.

34. Olver, F. W. J. 1974. Asymptotics and Special Functions. Academic Press, New York. 572 pp.

35. McLaughlin, S. 1989. The electrostatic properties of membranes. *Annu. Rev. Biophys. Biophys. Chem.* 18:113–136.

36. Bockris, J., and A. Reddy. 1970. Modern Electrochemistry. Vol. 1. Plenum Press, New York. 622 pp.

37. Barcilon, V., D. Chen, R. Eisenberg and M. Ratner. 1993. Barrier crossing with concentration boundary conditions in biological channels and chemical reactions. *J. Chem. Phys.* 98:1193–1212.

38. Mock, M. S. 1983. Analysis of Mathematical Models of Semiconductor Devices. Boole Press, Dublin. 197 pp.

39. Selberherr, S. 1984. Analysis and Simulation of Semiconductor Devices. Springer-Verlag, New York. 293 pp.

40. Markowich, P. A. 1986. The Stationary Semiconductor Device Equations. Springer-Verlag, New York. 193 pp.

41. Hodgkin, A. L. and W. K. Chandler. 1965. Effects of changes in ionic strength on inactivation and threshold in perfused nerve fibers of *Loligo. J. Gen. Physiol.* 48:27–30.

42. Rubinstein, I. 1987. Multiple steady-state solutions in one-dimensional electrodiffusion with local electroneutrality. *SIAM (Soc.*

Ind. Appl. Math.)-SIMS (SIAM Inst. Math. Soc.) Conf. Ser. 47:1076–1093.

43. Mock, M. 1982. An example of non-uniqueness of stationary solutions in semiconductor device models. COMPEL-International Journal for Computation and Mathematics in EEE 1:165–174.

44. Steinrück, H. 1989. A bifurcation analysis of one-dimensional steady-state semiconductor device equations. *SIAM (Soc. Ind. Appl. Math.)-SIMS (SIAM Inst. Math. Soc.) Conf. Ser.* 49:1102–1121.

45. Schulz, G. E., and R. H. Schirmer. 1979. Principles of Protein Structure. Springer Verlag, New York. 314 pp.

46. Baker, P. F., A. L. Hodgkin and H. Meves. 1964. The effect of diluting the internal solution on the electrical properties of a perfused giant axon. *J. Physiol. (Lond.)*. 170:541–560.

47. Chandler, W. K., A. L. Hodgkin, and H. Meves. 1965. The effect of changing the internal solution on sodium inactivation and related phenomena in giant axons. *J. Physiol. (Lond.)*. 180:821–836.

48. Wallace, B. A. 1990. Gramicidin channels and pores. *Annu. Rev. Biophys. Chem.* 19:127–157.

49. Eisenberg, R. S. 1990. Channels as enzymes. *J. Membr. Biol.* 115:1–12.

50. Jacobson, S. H., M. A. Ratner and A. Nitzan. 1983. Motion mechanisms in framework solid electrolytes: correlated hopping and liquidlike diffusion. *J. Chem. Phys.* 78:4154–4161.

51. Roux, B., and M. Karplus. 1991. Ion transport in a model gramicidin channel. *Biophys. J.* 59:961–981.

52. Frankenhaeuser, B., A. L. Hodgkin. 1957. The action of calcium on the electrical properties of squid axons. *J. Physiol. (Lond.)*. 137:218–244.

53. Green, W. N., and O. S. Andersen. 1991. Surface charges and ion channel function. *Annu. Rev. Physiol.* 53:341–359.

54. Hodgkin, A. L., and A. F. Huxley. 1952. A quantitative description of membrane current and its application to conduction and excitation in nerve. *J. Physiol. (Lond.)*. 117:500–544.

55. Frankenhaeuser, B. 1960. Sodium permeability in toad nerve and in squid nerve. *J. Physiol. (Lond.)*. 152:159–166.

56. Peskoff, A., and D. M. Bers. 1986. Electrodiffusion of ions approaching the mouth of a conducting membrane channel. *Biophys. J.* 53:863–875.

57. Dani, J. A. 1986. Ion channel entrances influence permeation: net charge, size, shape and binding considerations. *Biophys. J.* 49:607–618.

58. Gibbs, J. W. 1909. Vector Analysis. Dover Publications, reprinted in 1960, New York. 436 pp.

59. Crowe, M. J. 1985. A History of Vector Analysis. Dover Publications, New York. 270 pp.

60. Altmann, S. L. 1986. Rotations, Quaternions, and Double Groups. Clarendon Press, Oxford, UK. 317 pp.

61. Creighton, T. E. 1983. Proteins: Structures and Molecular Properties. W. H. Freeman & Co., New York. 515 pp.

62. Cowley, J. M. 1984. Diffraction Physics. North Holland. 430 pp.

63. Stratton, J. A. 1941. Electromagnetic Theory. McGraw-Hill Publishing, New York. 615 pp.

64. Hodgkin, A. L. 1958. Ionic movements and electrical activity in giant nerve fibers. *Proc. R. Soc. B Biol. Sci.* 148:1–37.

65. Heaviside, O. 1886, reprinted in 1970. Electrical Papers. Vol. 1. 2nd ed. Chelsea Publishing Co., New York.

66. Nahin, P. J. 1987. Oliver Heaviside: Sage in Solitude. IEEE Press, New York. 320 pp.

67. Feynmann, R. P., R. B. Leighton, and M. Sands. 1963. The Feynman: Lectures on Physics. Vol. 1. Addison-Wesley Publishing Co., New York.

68. Gawrisch, K., D. Ruston, J. Zimmerberg, A. Parsegian, R. P. Rand, and N. Fuller. 1992. Membrane dipole potentials, hydration forces, and the ordering of water at membrane surfaces. *Biophys. J.* 61:1213–1223.